A posteriori error analysis of an enriched Galerkin method of order one for the Stokes problem

Vivette Girault, Frédéric Hecht, Taboada Maria Gonzalez

▶ To cite this version:

Vivette Girault, Frédéric Hecht, Taboada Maria Gonzalez. A posteriori error analysis of an enriched Galerkin method of order one for the Stokes problem. Journal of Numerical Mathematics, inPress. hal-03867869

HAL Id: hal-03867869

https://hal.science/hal-03867869v1

Submitted on 23 Nov 2022

HAL is a multi-disciplinary open access archive for the deposit and dissemination of scientific research documents, whether they are published or not. The documents may come from teaching and research institutions in France or abroad, or from public or private research centers.

L'archive ouverte pluridisciplinaire **HAL**, est destinée au dépôt et à la diffusion de documents scientifiques de niveau recherche, publiés ou non, émanant des établissements d'enseignement et de recherche français ou étrangers, des laboratoires publics ou privés.

Research article

Vivette Girault, María González*, and Frédéric Hecht

A posteriori error analysis of an enriched Galerkin method of order one for the Stokes problem

https://doi.org/..., Received ; accepted

Abstract: We derive optimal reliability and efficiency of a posteriori error estimates for the steady Stokes problem, with a nonhomogeneous Dirichlet boundary condition, solved by a stable enriched Galerkin scheme (EG) of order one on triangular or quadrilateral meshes in $\mathbb{R}^2$, and tetrahedral or hexahedral meshes in $\mathbb{R}^3$.

Keywords: Steady Stokes system, nonhomogeneous Dirichlet boundary condition, enriched Galerkin scheme, reliable and efficient residual a posteriori estimates

MSC: 65N15, 65N30, 65N50, 76D07

Communicated by:
Dedicated to

1 Introduction

In the recent paper [10], a new stable enriched Galerkin element for the Stokes problem was introduced and analyzed. In this element, the pressure is approximated by piecewise constants and the velocity is approximated by continuous linear polynomials (in the simplicial case) plus piecewise constants. As usual, in the case of quadrilateral or hexahedral elements, to achieve continuity, the linear polynomials are replaced by the inverse images of bilinear or trilinear elements according to the dimension. As is shown in [10], this pair of spaces satisfies a uniform inf-sup condition both in two and three dimensions on simplices and on quadrilaterals or plane faced hexahedra. The a priori analysis shows that it has order one. This scheme can be easily implemented and can be used to solve large problems. Of course, it involves

Vivette Girault, Frédéric Hecht, Laboratoire Jacques-Louis Lions, Sorbonne Université.
***Corresponding author: María González,** Departamento de Matemáticas and CITIC, Universidade da Coruña.

jumps because of the piecewise velocity constants, but compared to first-order standard discontinuous Galerkin methods, see for instance [29], it requires less degrees of freedom (DOFs, see Figure 1) and its computer implementation is easier because the jumps are constant functions. Compared to the first-order Crouzeix-Raviart element, see [14], it has the advantage of applying to quadrilaterals and hexahedra. And compared to the rotated quadrilateral or hexahedral element of order one, see [28], it does not lose accuracy when the element is distorted.

The idea of adding piecewise constants to continuous finite element methods has been used first by Becker et al. [5] and Sun and Liu [31] for solving elliptic problems. It has been further studied by Lee et al. in [24] for parabolic problems and applied in [25, 26, 27] to geomechanics problems.

The literature on a posteriori error analysis of the Stokes equations is very extensive. Up to our knowledge, the first work is [32], where two reliable and locally efficient a posteriori error estimators are proposed and analyzed for the mini-element. One is an explicit residual-based estimator and the other is based on the solution of suitable local Stokes problems. The latter is simplified in [4]. Ainsworth and Oden [2] proposed an a posteriori error estimator based on the solution of local Poisson residual problems. This error estimator provides a guaranteed upper bound on the true error in an energy-like norm, and the analysis is valid for essentially any finite element approximation, including h-p finite elements.

In [6] the Stokes problem is solved by adding a penalty parameter to the saddle point variational formulation; the penalized problem is then solved by the finite element method. The authors presented two types of error indicators: one related to the penalty term and the other to the finite element discretization. Anisotropic finite element discretizations were considered in [13]. That analysis covers conforming and non-conforming discretizations and some of their results are new for isotropic meshes.

Dörfler and Ainsworth [16] proposed fully computable explicit a posteriori error estimates for the lowest order nonconforming Crouzeix-Raviart element provided that a reasonable lower bound for the inf-sup constant is available. A computational survey of a posteriori error estimators for that element can be found in [9]. Local a posteriori error estimates for the gradient of the velocity field in the maximum error for the standard Hood-Taylor discretization are analyzed in [15]. More recently, a posteriori error estimators for classical low-order inf-sup stable finite element discretizations of the Stokes problem with singular sources are presented in [3].

Regarding the a posteriori error analysis of mixed discontinuous Galerkin methods, the first computable upper bounds on the error, measured in terms of a mesh-dependent energy-norm, appear to be [21]. Anisotropic residual a posteriori error estimators were proposed in [12].

The aim of this paper is to develop the a posteriori error analysis of the method introduced in [10]. Our error indicators are residual-based; we study both reliability and efficiency of the indicators, and the results in both cases are optimal. Because of the discontinuous constants, the analysis shares some aspects with those of discontinuous Galerkin methods (DG), see for example [23], but it also differs in the approximation of the divergence because it includes an additional stabilizing term.

This article is organized as follows. In the remaining part of this Section we introduce some notation to be used throughout the paper. In Section 2 we describe the model problem. We present the associated enriched Galerkin scheme in Section 3. Section 4 is the core of the paper: we first derive error equalities for the velocity and the pressure; then, we derive the corresponding error inequalities and establish the reliability and local efficiency of the proposed a posteriori error indicator. In Section 5 we report some numerical results. Finally, we discuss in the Appendix the extension to the case of non planar hexahedra, an approximation of the boundary data, and the choice of the penalty parameters.

1.1 Notation

Let $\Omega \subset \mathbb{R}^d$ $(d = 2\,,3)$ be a bounded domain with boundary Γ. For any real number $p \geq 1$, $L^p(\Omega)$ is the Lebesgue space of measurable functions v such that $|v|^p$ is integrable in Ω, normed by

$$\|v\|_{L^p(\Omega)} = \Big(\int_\Omega |v|^p \Big)^{\frac{1}{p}}.$$

The space $L^2(\Omega)$ is a Hilbert space for the associated scalar product

$$(u, v) = \int_\Omega u\, v.$$

We denote by $L^2_0(\Omega)$ the subspace of functions of $L^2(\Omega)$ with zero mean in Ω,

$$L^2_0(\Omega) = \{v \in L^2(\Omega) \,:\, \int_\Omega v = 0\},$$

with the same norm and scalar product.

We denote by $H^1(\Omega)$ the Sobolev space of functions in $L^2(\Omega)$ with first order partial derivatives (in the distributional sense) in $L^2(\Omega)$:

$$H^1(\Omega) = \{v \in L^2(\Omega) \,:\, \nabla\, v \in [L^2(\Omega)]^d\},$$

and by $H_0^1(\Omega)$ the subspace of functions in $H^1(\Omega)$ that vanish on its boundary Γ. The norm of $H^1(\Omega)$ is

$$\|v\|_{H^1(\Omega)} = \left(\|v\|^2_{L^2(\Omega)} + |v|^2_{H^1(\Omega)}\right)^{\frac{1}{2}},$$

where $|\cdot|$ denotes the seminorm,

$$|v|_{H^1(\Omega)} = \|\nabla v\|_{[L^2(\Omega)]^d},$$

which is a Hilbert norm for $H_0^1(\Omega)$ owing to the Poincaré inequality. More generally, $W^{1,p}(\Omega)$ is the Sobolev space

$$W^{1,p}(\Omega) = \{v \in L^p(\Omega) \,:\, \nabla v \in [L^p(\Omega)]^d\},$$

normed by

$$\|v\|_{W^{1,p}(\Omega)} = \left(\|v\|^p_{L^p(\Omega)} + |v|^p_{W^{1,p}(\Omega)}\right)^{\frac{1}{p}},$$

where

$$|v|^p_{W^{1,p}(\Omega)} = \|\nabla v\|^p_{[L^p(\Omega)]^d}.$$

We denote by $H^{1/2}(\Gamma)$ the space of traces on Γ of functions in $H^1(\Omega)$. When Γ is a portion of the boundary with non zero measure, we denote by $H^{1/2}_{00}(\Gamma)$ the subspace of functions of $H^{1/2}(\Gamma)$, that when extended by zero to the whole boundary $\partial\Omega$ still belong to $H^{1/2}(\partial\Omega)$. We shall use here the intrinsic seminorm of $H^{1/2}(\Gamma)$,

$$|v|_{H^{1/2}(\Gamma)} := \Big(\int_\Gamma \int_\Gamma \frac{|v(\mathbf{x}) - v(\mathbf{y})|^2}{|\mathbf{x} - \mathbf{y}|^d} d\mathbf{x}\, d\mathbf{y}\Big)^{\frac{1}{2}},$$

and the norm of $H^{1/2}_{00}(\Gamma)$,

$$\|v\|_{H^{1/2}_{00}(\Gamma)} = \left(\|v\|^2_{L^2(\Gamma)} + |v|^2_{H^{1/2}(\Gamma)} + \int_\Gamma |v(\mathbf{x})|^2 \,\frac{d\mathbf{x}}{d(\mathbf{x}, \partial\Gamma)}\right)^{\frac{1}{2}},$$

where $d(\mathbf{x}, \partial\Gamma)$ denotes the distance function to the boundary of Γ. See [1] for the definitions of fractional Sobolev spaces $H^s(\Omega)$, for real numbers $s > 0$. Finally, given a Hilbert space H, we denote by H^d and $H^{d\times d}$, respectively, the vector and tensor versions of H. Given two second-order tensors, $\boldsymbol{\sigma}$ and $\boldsymbol{\tau}$, we denote its inner product by

$$\boldsymbol{\sigma} : \boldsymbol{\tau} = \sum_{i,j=1}^{d} \sigma_{ij}\tau_{ij}\,.$$

2 Model problem

We consider a bounded domain $\Omega \subset \mathbb{R}^d$ ($d = 2, 3$) with a Lipschitz-continuous boundary $\Gamma := \partial\Omega$, filled with a fluid. Recall that by definition a domain is open and connected. We denote by $\mathbf{n}$ the unit outward normal to Γ. Let $\mathbf{f} \in [L^2(\Omega)]^d$ be a volume force, $\mathbf{g}_D \in [H^{1/2}(\Gamma)]^d$ be a prescribed velocity such that

$$\int_\Gamma \mathbf{g}_D \cdot \mathbf{n} = 0\,, \tag{1}$$

and let $\mu > 0$ denote the fluid viscosity, assumed to be constant. We consider the Stokes problem: find the fluid velocity $\mathbf{u} : \Omega \to \mathbb{R}^d$ and the fluid pressure $p : \Omega \to \mathbb{R}$ such that

$$\begin{cases} -\mu\,\Delta\mathbf{u} + \nabla p = \mathbf{f} & \text{in } \Omega\,,\\ \nabla\cdot\mathbf{u} = 0 & \text{in } \Omega\,,\\ \mathbf{u} = \mathbf{g}_D & \text{on } \Gamma\,,\\ \int_\Omega p = 0\,, & \end{cases} \tag{2}$$

where the last condition is introduced to guarantee uniqueness of the pressure.

It is well-known that the following inf-sup condition holds; there is a positive constant β such that

$$\inf_{q\in L^2_0(\Omega)} \sup_{\mathbf{v}\in[H^1_0(\Omega)]^d} \frac{-\int_\Omega q\,\nabla\cdot\mathbf{v}}{|\mathbf{v}|_{[H^1(\Omega)]^d}\|q\|_{L^2(\Omega)}} \geq \beta\,, \tag{3}$$

and problem (2) has a unique solution $(\mathbf{u}, p)$ in $[H^1(\Omega)]^d \times L^2_0(\Omega)$, cf. for instance [19]. In fact, it suffices that $\mathbf{f}$ belongs to $[H^{-1}(\Omega)]^d$, the dual space of $[H^1_0(\Omega)]^d$, but we restrict the discussion to forces in $[L^2(\Omega)]^d$ because below $\mathbf{f}$ will be applied to functions that do not have H^1 regularity.

3 Discretization

From now on, we restrict the discussion to the case when Ω is a bounded connected polygon in $\mathbb{R}^2$ or Lipschitz polyhedron in $\mathbb{R}^3$. This restriction substantially simplifies the analysis and implementation owing that it avoids curved faces on the boundary and their possible approximation. But in the case of hexahedra, it does not necessarily rule out interior curved faces, even though all their edges are straight lines. For the sake or simplicity, we shall only deal with *planar faces* hexahedra and postpone to the appendix a brief study of an extension to curved-faced hexahedra.

3.1 Mesh and discrete spaces

Let $\mathcal{T}_h$ be a partition of $\overline{\Omega}$ made up of triangles or quadrilaterals ($d = 2$) and tetrahedra or hexahedra ($d = 3$). Given an element $E \in \mathcal{T}_h$, we denote by h_E the diameter of E, and by $h = \max_{E\in\mathcal{T}_h} h_E$. We assume that $\mathcal{T}_h$ is a regular family of meshes in the following sense:

1. In the case of simplices, $\mathcal{T}_h$ is regular as defined by Ciarlet [11].
2. In the case of quadrilaterals, when dividing each quadrilateral into two subtriangles by any diagonal, the resulting triangular mesh is regular in the sense of Ciarlet, see for example [19].
3. In the case of hexahedra, the mapping from the reference element $\hat{E}$ (unit square or cube according to the dimension) to any physical element E is invertible at all points of $\hat{E}$ and its Jacobian determinant is bounded below by $c\,h^3$ with a constant c independent of h and E.

This definition implies in particular that all elements are convex. But whereas for quadrilaterals, the notion of regularity reduces to a simple geometrical property, this is not yet known for hexahedra, even in the simpler case of planar hexahedra, see [22].

We denote by $\mathcal{E}_h$ the set of all edges ($d = 2$) or faces ($d = 3$) of $\mathcal{T}_h$; $\mathcal{E}_h^0$ denotes the set of all interior edges (resp., faces) and $\mathcal{E}_h^\partial$ is the set of all boundary edges (resp., faces), so that

$$\mathcal{E}_h = \mathcal{E}_h^0 \cup \mathcal{E}_h^\partial.$$

To simplify, it is convenient to use the following notation:

$$\int_{\mathcal{T}_h} := \sum_{E\in\mathcal{T}_h} \int_E, \qquad \int_{\mathcal{E}_h} := \sum_{e\in\mathcal{E}_h} \int_e, \qquad \int_{\mathcal{E}_h^0} := \sum_{e\in\mathcal{E}_h^0} \int_e, \qquad \int_{\mathcal{E}_h^\partial} := \sum_{e\in\mathcal{E}_h^\partial} \int_e .$$

Given an edge or face $e \in \mathcal{E}_h$, h_e denotes its $(d-1)$-dimensional measure.

Now, let $k \geq 1$ be an integer. For a simplex $E \in \mathcal{T}_h$, we let $\mathcal{P}_k(E)$ denote the space of polynomials of degree at most k in E. In the case of E, quadrilateral ($d = 2$) or hexahedron ($d = 3$), $\mathcal{P}_k(E)$ is defined as the inverse image of $Q_k(\hat{E})$, where $\hat{E}$ is the reference element and $Q_k(\hat{E})$ is the space of polynomials of degree k in *each* variable,

$$\mathcal{P}_k(E) = \{q = \hat{q} \circ \mathcal{F}^{-1} \,:\, \hat{q} \in Q_k(\hat{E})\}, \tag{4}$$

where $\mathcal{F}$ is a one-to-one bilinear ($d=2$) or trilinear ($d=3$) mapping of $\hat{E}$ onto E; its existence is guaranteed by the regularity of the mesh. Note that, when E is a simplex, the space defined by (4) coincides with that of polynomials of degree at most k in E. Note also that, unless E is a parallelogram ($d=2$) or parallelepiped ($d=3$), the functions defined by (4) are in general not polynomials. Finally, when $k=0$, $\mathcal{P}_0(E)$ is the space of constant functions in all elements whatever their shape.

Let $M^k(\mathcal{T}_h)$ be the space of piecewise discontinuous functions $\mathcal{P}_k(E)$ in each E:

$$M^k(\mathcal{T}_h) := \{v \in L^2(\Omega) \,:\, v_{|E} \in \mathcal{P}_k(E)\,, \quad \forall\, E \in \mathcal{T}_h\}\,. \tag{5}$$

We then define the space of globally continuous functions that are $\mathcal{P}_k(E)$ in each E:

$$M_0^k(\mathcal{T}_h) := M^k(\mathcal{T}_h) \cap H^1(\Omega)\,.$$

The enriched Galerkin finite element space is the space of discontinuous functions:

$$V_{h,k}^{EG} := M_0^k(\mathcal{T}_h) \,+\, M^0(\mathcal{T}_h)\,, \qquad k \geq 1\,. \tag{6}$$

Now, we associate a unit normal vector $\mathbf{n}_e$ to each edge or face $e \in \mathcal{E}_h$, with arbitrary but fixed orientation, and with the convention that $\mathbf{n}_e = \mathbf{n}$ is the unit outward normal to the boundary Γ when $e \in \mathcal{E}_h^\partial$. Let E^- and E^+ be the two elements sharing an edge or face $e \in \mathcal{E}_h^0$, such that $\mathbf{n}_e$ points from E^- to E^+. Given smooth functions $q : \mathcal{T}_h \to \mathbb{R}$, for instance $q \in W^{1,1}(\mathcal{T}_h)$, and $\mathbf{v} : \mathcal{T}_h \to \mathbb{R}^d$, $\mathbf{v} \in [W^{1,1}(\mathcal{T}_h)]^d$, we define their *average*, $\{\cdot\}_{|e}$, and *jump*, $[\cdot]_{|e}$, on e as follows:

$$\{q\}_{|e} = \frac{1}{2}\left((q_{|E^-})_{|e} + (q_{|E^+})_{|e}\right), \qquad [q]_{|e} = \left((q_{|E^-})_{|e} - (q_{|E^+})_{|e}\right),$$
$$\{\mathbf{v}\}_{|e} = \frac{1}{2}\left((\mathbf{v}_{|E^-})_{|e} + (\mathbf{v}_{|E^+})_{|e}\right), \qquad [\mathbf{v}]_{|e} = \left((\mathbf{v}_{|E^-})_{|e} - (\mathbf{v}_{|E^+})_{|e}\right).$$

Here $W^{1,1}(\mathcal{T}_h)$ denotes the space of functions v in $L^1(\Omega)$ such that for each E of $\mathcal{T}_h$, $v|_E$ belongs to $W^{1,1}(E)$. On boundary edges or faces $e \in \mathcal{E}_h^\partial$, the average and jump of any function q or $\mathbf{v}$ are simply replaced by the trace of this function on e. With this notation, we choose for $V_{h,k}^{EG}$ the usual DG norm,

$$\|\mathbf{v}_h\|_{EG}^2 := \int_{\mathcal{T}_h} \nabla \mathbf{v}_h \,:\, \nabla \mathbf{v}_h \,+\, \int_{\mathcal{E}_h} \frac{\sigma_e}{h_e}\,[\mathbf{v}_h]\cdot[\mathbf{v}_h]\,, \tag{7}$$

and the seminorm,

$$|\mathbf{v}_h|_h = \Big(\int_{\mathcal{T}_h} \nabla \mathbf{v}_h \,:\, \nabla \mathbf{v}_h\Big)^{\frac{1}{2}}.$$

Here σ_e are nonnegative penalty parameters defined on each edge (resp., face) to be chosen further on (see subsection 6.2). If the usual DG norm defined in (7) is restricted to a macroelement S, we will indicate it as $\|\cdot\|_{EG,S}$. The discrete velocity will be found in $[V_{h,k}^{EG}]^d$ for $k=1$, and the discrete pressure in $M^0(\mathcal{T}_h)$. As expected, the norm of $M^0(\mathcal{T}_h)$ is the L^2-norm.

For $k=1$, the following Figure 1 shows the number of degrees of freedom (DOFs) of the scheme below using EG compared with standard DG. The numbers -3 and -4 in EG are due to the mean value constraint in the pressure and the fact that each component of the EG velocity has an extra constant function. To compute the asymptotic number of DOFs in three dimensions, we use the fact that in a classical tetrahedral mesh the number of tetrahedra is approximately six times the number of vertices. In a classical two dimensional triangular mesh, this factor is two.

Fig. 1: Comparison of DOFs for EG and classical DG for the Stokes problem with k=1. $\mathcal{N}_t$ and $\mathcal{N}_v$ are, respectively, the number of elements and the number of vertices in a simplicial triangulation.

	DG	**EG**
2d	$7\mathcal{N}_t - 1$	$2\mathcal{N}_v + 3\mathcal{N}_t - 3$
3d	$13\mathcal{N}_t - 1$	$3\mathcal{N}_v + 4\mathcal{N}_t - 4$

(a) Exact number of DOFs.

	DG	**EG**
2d	$14\mathcal{N}_v$	$8\mathcal{N}_v$
3d	$78\mathcal{N}_v$	$27\mathcal{N}_v$

(b) Asymptotic number of DOFs.

3.2 The enriched Galerkin scheme

We consider the enriched Galerkin method proposed in [10] for the Stokes problem with the choice $k=1$: find $\mathbf{u}_h \in [V_{h,k}^{EG}]^d$ and $p_h \in M^0(\mathcal{T}_h) \cap L_0^2(\Omega)$ such that

$$\begin{cases} \mu\, a_\epsilon(\mathbf{u}_h, \mathbf{v}_h) + b(\mathbf{v}_h, p_h) = L(\mathbf{v}_h)\,, & \forall\, \mathbf{v}_h \in [V_{h,k}^{EG}]^d\,, \\ b(\mathbf{u}_h, q_h) = G(q_h)\,, & \forall\, q_h \in M^0(\mathcal{T}_h) \cap L_0^2(\Omega)\,, \end{cases} \tag{8}$$

where for any $\mathbf{u}_h$, $\mathbf{v}_h \in [V_{h,k}^{EG}]^d$ and $q_h \in M^0(\mathcal{T}_h) \cap L_0^2(\Omega)$,

$$\begin{aligned} a_\epsilon(\mathbf{u}_h, \mathbf{v}_h) \quad &:= \int_{\mathcal{T}_h} \nabla \mathbf{u}_h : \nabla \mathbf{v}_h - \int_{\mathcal{E}_h} \{\nabla \mathbf{u}_h \, \mathbf{n}_e\} \cdot [\mathbf{v}_h] \\ &+ \quad \epsilon \int_{\mathcal{E}_h} [\mathbf{u}_h] \cdot \{\nabla \mathbf{v}_h \, \mathbf{n}_e\} + \int_{\mathcal{E}_h} \frac{\sigma_e}{h_e} [\mathbf{u}_h] \cdot [\mathbf{v}_h] , \end{aligned} \tag{9}$$

$$b(\mathbf{v}_h, q_h) := - \int_{\mathcal{T}_h} q_h \, \nabla \cdot \mathbf{v}_h + \int_{\mathcal{E}_h} \{q_h\} \, [\mathbf{v}_h] \cdot \mathbf{n}_e + \alpha \int_{\mathcal{E}_h^0} [\mathbf{v}_h] \cdot \mathbf{n}_e \, [q_h] , \tag{10}$$

$$L(\mathbf{v}_h) := \int_{\mathcal{T}_h} \mathbf{f} \cdot \mathbf{v}_h + \epsilon\mu \int_{\mathcal{E}_h^\partial} (\nabla \mathbf{v}_h \, \mathbf{n}) \cdot \mathbf{g}_D + \mu \int_{\mathcal{E}_h^\partial} \frac{\sigma_e}{h_e} \mathbf{v}_h \cdot \mathbf{g}_D , \tag{11}$$

and

$$G(q_h) := \int_{\mathcal{E}_h^\partial} q_h \, \mathbf{g}_D \cdot \mathbf{n} . \tag{12}$$

The form $a_\epsilon(\cdot,\cdot)$ is the usual DG approximation of $(\nabla \mathbf{u}, \nabla \mathbf{v})$. Depending on the choice of ϵ, we have different algorithms. For example, for $\epsilon = -1$, we recover the *Symmetric Interior Penalty Galerkin* (*SIPG*) method; for $\epsilon = 1$, we recover the *Non-symmetric Interior Penalty Galerkin* (*NIPG*) method, and for $\epsilon = 0$, we have the *Incomplete Interior Penalty Galerkin* (*IIPG*) method. The penalty parameters σ_e are chosen large enough (usually larger than one), independent of h, to guarantee that the bilinear form $a_\epsilon(\cdot,\cdot)$ is elliptic. The form $b(\cdot,\cdot)$ is not the usual DG approximation of $(q, \nabla \cdot \mathbf{v})$. Its last term is a consistent term introduced to satisfy a discrete inf-sup condition, at least when $k = 1$. It is consistent for all values of the parameter α, but it is used here with $\alpha = \pm\frac{1}{2}$, because for these values the following discrete inf-sup condition is satisfied when $k = 1$:

$$\inf_{q_h \in M^0(\mathcal{T}_h)} \sup_{\mathbf{v}_h \in [V_{h,k,0}^{EG}]^d} \frac{b(\mathbf{v}_h, q_h)}{\|\mathbf{v}_h\|_{EG} \|q_h\|_{L^2(\Omega)}} \geq \beta^\star , \tag{13}$$

for a constant $\beta^\star > 0$, independent of h, where

$$V_{h,k,0}^{EG} = M^k(\mathcal{T}_h) \cap H_0^1(\Omega) + M^0(\mathcal{T}_h).$$

It is shown in [10], in the case of triangles, quadrilaterals, tetrahedra and planar hexahedra, that (13) holds when no element has more than three when $d = 3$ (or two when $d = 2$) interior normals and no pair of interior normals is located on opposite faces of quadrilaterals or hexahedra (see Figure 3.2), whence problem (8) has exactly one solution. This mild restriction concerns only interior faces because the normal to Γ always points outside the domain. It was found to be directly satisfied in all our numerical experiments on simplicial meshes, owing to a suitable numbering of the elements. It can also be easily checked on quadrilateral or hexahedral meshes with cartesian numbering.

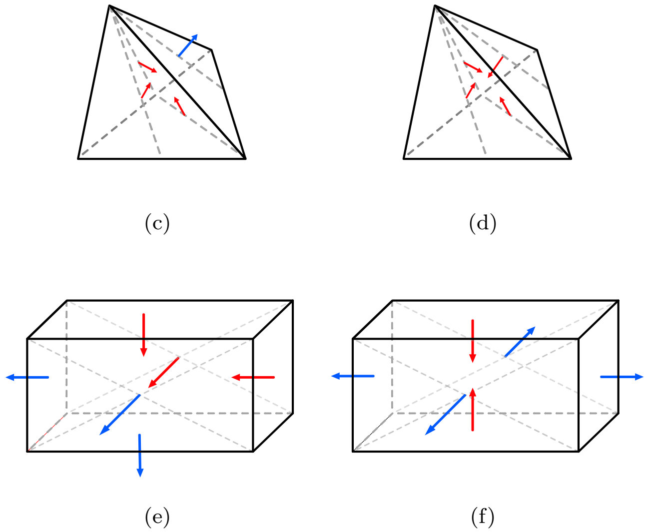

Fig. 2: Cases (a) and (c) illustrate two possible choices of the normals. Cases (b) and (d) do not meet the assumptions.

In the next section we develop an a posteriori error analysis for the SIPG method. The analysis for the NIPG and IIPG methods is somewhat simpler but follows the same steps.

In what follows we assume that the boundary data $\mathbf{g}_D$ is the trace of a function of $[M_0^k(\mathcal{T}_h)]^d$ satisfying (1). This simplifying assumption is discussed in subsection 6.1.

4 A posteriori error analysis for the symmetric interior penalty enriched Galerkin method

Motivated by the discrete inf-sup condition, the analysis below addresses the case $k = 1$ and $\alpha = \pm\frac{1}{2}$, but it easily extends to arbitrary k and α except when the inf-sup condition is needed. In this section, we shall first derive error equalities adapted to a posteriori estimates, then deduce from these the expression of error indicators and establish reliability bounds. The local efficiency of the error indicators is derived at the end.

4.1 Error equalities

In this section, we choose $\epsilon = -1$. We further assume that the exact solution is somewhat smoother: $(\mathbf{u}, p) \in [H^{1+s}(\Omega)]^d \times H^s(\Omega)$, for some $s > 0$, so that the terms in (14) and (15) below are all meaningful. This additional regularity for $\mathbf{u}$ is compatible with the assumption that $\mathbf{g}_D$ is the trace of a function of $[M_0^k(\mathcal{T}_h)]^d$, provided $0 < s < \frac{1}{2}$; this is not a constraint since $s > 0$ is supposed to be small. The following properties hold, namely, Galerkin orthogonality:

$$\mu\, a_{-1}(\mathbf{u} - \mathbf{u}_h, \mathbf{v}_h) + b(\mathbf{v}_h, p - p_h) = 0 \quad \forall\, \mathbf{v}_h \in [V_{h,k}^{EG}]^d\,, \tag{14}$$

and consistency:

$$\begin{aligned} \mu\, a_{-1}(\mathbf{u}, \mathbf{v} - \mathbf{v}_h) + b(\mathbf{v} - \mathbf{v}_h, p) &= \int_{\mathcal{T}_h} \mathbf{f} \cdot (\mathbf{v} - \mathbf{v}_h) \\ +\mu \int_{\mathcal{E}_h^\partial} \frac{\sigma_e}{h_e}\, \mathbf{g}_D \cdot (\mathbf{v} - \mathbf{v}_h) &- \mu \int_{\mathcal{E}_h^\partial} \mathbf{g}_D \cdot (\nabla(\mathbf{v} - \mathbf{v}_h)\, \mathbf{n}) \quad \forall\, \mathbf{v}_h \in [V_{h,k}^{EG}]^d\,, \end{aligned} \tag{15}$$

for all $\mathbf{v}$ sufficiently smooth so that all terms above are well defined.

With the intention of deriving the velocity error equation, we first use the Galerkin orthogonality property (14),

$$\mu\, a_{-1}(\mathbf{u} - \mathbf{u}_h, \mathbf{v}) + b(\mathbf{v}, p - p_h) = \mu\, a_{-1}(\mathbf{u} - \mathbf{u}_h, \mathbf{v} - \mathbf{v}_h) + b(\mathbf{v} - \mathbf{v}_h, p - p_h)\,.$$

Then, by using the consistency property (15),

$$\mu\, a_{-1}(\mathbf{u}-\mathbf{u}_h,\mathbf{v}) + b(\mathbf{v},p-p_h) =$$

$$= \mu\, a_{-1}(\mathbf{u},\mathbf{v}-\mathbf{v}_h) + b(\mathbf{v}-\mathbf{v}_h,p) - \mu\, a_{-1}(\mathbf{u}_h,\mathbf{v}-\mathbf{v}_h) - b(\mathbf{v}-\mathbf{v}_h,p_h)$$
$$= \int_{\mathcal{T}_h} \mathbf{f}\cdot(\mathbf{v}-\mathbf{v}_h) + \mu \int_{\mathcal{E}_h^\partial} \frac{\sigma_e}{h_e}\mathbf{g}_D\cdot(\mathbf{v}-\mathbf{v}_h) - \mu\int_{\mathcal{E}_h^\partial} \mathbf{g}_D\cdot(\nabla(\mathbf{v}-\mathbf{v}_h)\,\mathbf{n})$$
$$-\mu\, a_{-1}(\mathbf{u}_h,\mathbf{v}-\mathbf{v}_h) - b(\mathbf{v}-\mathbf{v}_h,p_h).$$

Therefore, by inserting any piecewise polynomial function $\mathbf{f}_h$,

$$\mu\, a_{-1}(\mathbf{u}-\mathbf{u}_h,\mathbf{v}) + b(\mathbf{v},p-p_h) =$$
$$= \int_{\mathcal{T}_h} (\mathbf{f}-\mathbf{f}_h)\cdot(\mathbf{v}-\mathbf{v}_h) + \int_{\mathcal{T}_h} \mathbf{f}_h\cdot(\mathbf{v}-\mathbf{v}_h)$$
$$+\mu \int_{\mathcal{E}_h^\partial} \frac{\sigma_e}{h_e}\mathbf{g}_D\cdot(\mathbf{v}-\mathbf{v}_h) - \mu\int_{\mathcal{E}_h^\partial} \mathbf{g}_D\cdot(\nabla(\mathbf{v}-\mathbf{v}_h)\,\mathbf{n})$$
$$-\mu\, a_{-1}(\mathbf{u}_h,\mathbf{v}-\mathbf{v}_h) - b(\mathbf{v}-\mathbf{v}_h,p_h)\,.$$

Using Green's formula in the volume integrals of $a_{-1}(\mathbf{u}_h,\mathbf{v}-\mathbf{v}_h)$ and $b(\mathbf{v}-\mathbf{v}_h,p_h)$, we arrive at the following error equation for all $\mathbf{v}$ sufficiently smooth and all $\mathbf{v}_h \in [V_{h,k}^{EG}]^d$:

$$\mu\, a_{-1}(\mathbf{u}-\mathbf{u}_h,\mathbf{v}) + b(\mathbf{v},p-p_h) =$$
$$\begin{aligned}
&= \int_{\mathcal{T}_h} (\mathbf{f}-\mathbf{f}_h)\cdot(\mathbf{v}-\mathbf{v}_h) + \int_{\mathcal{T}_h} (\mathbf{f}_h + \mu\Delta\mathbf{u}_h - \nabla p_h)\cdot(\mathbf{v}-\mathbf{v}_h)\\
&+ \int_{\mathcal{E}_h^0} [(-\mu\nabla\mathbf{u}_h + p_h\mathbf{I})\mathbf{n}_e]\cdot\{\mathbf{v}-\mathbf{v}_h\} + \mu\int_{\mathcal{E}_h^0}\{\nabla(\mathbf{v}-\mathbf{v}_h)\mathbf{n}_e\}\cdot[\mathbf{u}_h]\\
&-\mu\int_{\mathcal{E}_h^0} \frac{\sigma_e}{h_e}\,[\mathbf{u}_h]\cdot[\mathbf{v}-\mathbf{v}_h] - \alpha\int_{\mathcal{E}_h^0}[(\mathbf{v}-\mathbf{v}_h)\cdot\mathbf{n}_e][p_h]\\
&+\mu\int_{\mathcal{E}_h^\partial} \frac{\sigma_e}{h_e}\,(\mathbf{g}_D-\mathbf{u}_h)\cdot(\mathbf{v}-\mathbf{v}_h) - \mu\int_{\mathcal{E}_h^\partial}(\mathbf{g}_D-\mathbf{u}_h)\cdot(\nabla(\mathbf{v}-\mathbf{v}_h)\,\mathbf{n})\,.
\end{aligned} \tag{16}$$

Now, by testing (16) with $\mathbf{v} = \mathbf{u} - \mathbf{u}_h$, and grouping interior and boundary terms, we obtain,

$$\begin{aligned}
&\mu\, a_{-1}(\mathbf{u}-\mathbf{u}_h, \mathbf{u}-\mathbf{u}_h) + b(\mathbf{u}-\mathbf{u}_h, p-p_h) = \\
&\quad = \int_{\mathcal{T}_h} (\mathbf{f}-\mathbf{f}_h)\cdot(\mathbf{u}-\mathbf{u}_h-\mathbf{v}_h) + \int_{\mathcal{T}_h} (\mathbf{f}_h + \mu\Delta\mathbf{u}_h - \nabla p_h)\cdot(\mathbf{u}-\mathbf{u}_h-\mathbf{v}_h) \\
&\quad + \int_{\mathcal{E}_h^0} [(-\mu\nabla\mathbf{u}_h + p_h\mathbf{I})\mathbf{n}_e]\cdot\{\mathbf{u}-\mathbf{u}_h-\mathbf{v}_h\} \\
&\quad + \mu\int_{\mathcal{E}_h} \{\nabla(\mathbf{u}-\mathbf{u}_h-\mathbf{v}_h)\mathbf{n}_e\}\cdot[\mathbf{u}_h-\mathbf{u}] \\
&\quad - \mu\int_{\mathcal{E}_h} \frac{\sigma_e}{h_e}[\mathbf{u}_h-\mathbf{u}]\cdot[\mathbf{u}-\mathbf{u}_h-\mathbf{v}_h] - \alpha\int_{\mathcal{E}_h^0}[(\mathbf{u}-\mathbf{u}_h-\mathbf{v}_h)\cdot\mathbf{n}_e][p_h]\,.
\end{aligned}$$

By expanding the left-hand side, passing all terms other than the EG norm (7) to the right-hand side, and cancelling some terms, this becomes

$$\begin{aligned}
\mu\,\|\mathbf{u}-\mathbf{u}_h\|_{EG}^2 &= \int_{\mathcal{T}_h} (\mathbf{f}-\mathbf{f}_h)\cdot(\mathbf{u}-\mathbf{u}_h-\mathbf{v}_h) \\
&\quad + \int_{\mathcal{T}_h} (\mathbf{f}_h + \mu\Delta\mathbf{u}_h - \nabla p_h)\cdot(\mathbf{u}-\mathbf{u}_h-\mathbf{v}_h) - \int_{\mathcal{T}_h} (\nabla\cdot\mathbf{u}_h)(p-p_h) \\
&\quad + \int_{\mathcal{E}_h^0} [(-\mu\nabla\mathbf{u}_h + p_h\mathbf{I})\mathbf{n}_e]\cdot\{\mathbf{u}-\mathbf{u}_h-\mathbf{v}_h\} \\
&\quad - \mu\int_{\mathcal{E}_h} \{\nabla(\mathbf{u}-\mathbf{u}_h+\mathbf{v}_h)\mathbf{n}_e\}\cdot[\mathbf{u}_h-\mathbf{u}] + \alpha\int_{\mathcal{E}_h^0}[\mathbf{v}_h\cdot\mathbf{n}_e][p_h] \\
&\quad - \mu\int_{\mathcal{E}_h} \frac{\sigma_e}{h_e}[\mathbf{u}_h-\mathbf{u}]\cdot[\mathbf{u}-\mathbf{u}_h-\mathbf{v}_h] + \int_{\mathcal{E}_h}\{p-p_h\}[(\mathbf{u}_h-\mathbf{u})\cdot\mathbf{n}_e]\,.
\end{aligned} \tag{17}$$

Now, we observe that the terms,

$$-\mu\int_{\mathcal{E}_h}\{\nabla(\mathbf{u}-\mathbf{u}_h)\mathbf{n}_e\}\cdot[\mathbf{u}_h-\mathbf{u}] \quad \text{and} \quad \int_{\mathcal{E}_h}\{p-p_h\}[(\mathbf{u}_h-\mathbf{u})\cdot\mathbf{n}_e]\,,$$

cannot be controlled by the left-hand side of (17), a situation common to DG schemes. In order to control these terms, inspired by the strategy in [23], we introduce a function $\mathbf{w} \in [M_0^k(\mathcal{T}_h)]^d$ such that $\mathbf{w} = \mathbf{g}_D$ on Γ, that does not jump across elements; here we use the assumption that $\mathbf{g}_D$ is the trace of a function of $[M_0^k(\mathcal{T}_h)]^d$. Then, we take $\mathbf{v}_h = \mathbf{u}_h - \mathbf{w}$ in (14):

$$\mu\, a_{-1}(\mathbf{u}-\mathbf{u}_h, \mathbf{u}_h-\mathbf{w}) + b(\mathbf{u}_h-\mathbf{w}, p-p_h) = 0\,. \tag{18}$$

Equation (18) reads:

$$\begin{aligned}\mu \int_{\mathcal{T}_h} \nabla(\mathbf{u}-\mathbf{u}_h) : \nabla(\mathbf{u}_h-\mathbf{w}) - \int_{\mathcal{T}_h} (p-p_h)\, \nabla\cdot(\mathbf{u}_h-\mathbf{w}) \\ + \mu \int_{\mathcal{E}_h} \frac{\sigma_e}{h_e} [\mathbf{u}-\mathbf{u}_h]\cdot[\mathbf{u}_h-\mathbf{w}] \\ - \mu \int_{\mathcal{E}_h} \{\nabla(\mathbf{u}-\mathbf{u}_h)\,\mathbf{n}_e\}\cdot[\mathbf{u}_h-\mathbf{w}] - \mu \int_{\mathcal{E}_h} [\mathbf{u}-\mathbf{u}_h]\cdot\{\nabla(\mathbf{u}_h-\mathbf{w})\,\mathbf{n}_e\} \\ + \int_{\mathcal{E}_h} \{p-p_h\}\,[\mathbf{u}_h-\mathbf{w}]\cdot\mathbf{n}_e + \alpha \int_{\mathcal{E}_h^0} [\mathbf{u}_h-\mathbf{w}]\cdot\mathbf{n}_e\,[p-p_h] = 0\,.\end{aligned}$$

Therefore, taking into account that $\mathbf{w}$ does not jump and that $\mathbf{w}=\mathbf{g}_D$ on Γ,

$$\begin{aligned}- \mu \int_{\mathcal{E}_h} \{\nabla(\mathbf{u}-\mathbf{u}_h)\,\mathbf{n}_e\}\cdot[\mathbf{u}_h-\mathbf{w}] + \int_{\mathcal{E}_h} \{p-p_h\}\,[\mathbf{u}_h-\mathbf{w}]\cdot\mathbf{n}_e = \\ = -\mu \int_{\mathcal{T}_h} \nabla(\mathbf{u}-\mathbf{u}_h) : \nabla(\mathbf{u}_h-\mathbf{w}) + \int_{\mathcal{T}_h} (p-p_h)\,\nabla\cdot(\mathbf{u}_h-\mathbf{w}) \\ + \mu \int_{\mathcal{E}_h} \frac{\sigma_e}{h_e} |[\mathbf{u}_h-\mathbf{u}]|^2 + \mu \int_{\mathcal{E}_h} [\mathbf{u}-\mathbf{u}_h]\cdot\{\nabla(\mathbf{u}_h-\mathbf{w})\,\mathbf{n}_e\} \\ - \alpha \int_{\mathcal{E}_h^0} [\mathbf{u}_h]\cdot\mathbf{n}_e\,[p-p_h]\,.\end{aligned} \tag{19}$$

Substituting (19) into (17) and taking $\mathbf{v}_h \in [V_{h,k}^{EG}]^d$ defined by

$$(\mathbf{v}_h)_{|E} = \frac{1}{|E|}\int_E (\mathbf{u}-\mathbf{u}_h) \qquad \forall\, E \in \mathcal{T}_h\,, \tag{20}$$

(so that $\nabla(\mathbf{v}_h)_{|E} = \mathbf{0}$ on every $E \in \mathcal{T}_h$), we obtain the velocity error equality:

$$\begin{aligned}
\mu \|\mathbf{u}-\mathbf{u}_h\|_{EG}^2 = &\int_{\mathcal{T}_h} (\mathbf{f}-\mathbf{f}_h)\cdot(\mathbf{u}-\mathbf{u}_h-\mathbf{v}_h)\\
&+\int_{\mathcal{T}_h} (\mathbf{f}_h+\mu\Delta\mathbf{u}_h-\nabla p_h)\cdot(\mathbf{u}-\mathbf{u}_h-\mathbf{v}_h) - \int_{\mathcal{T}_h} (\nabla\cdot\mathbf{u}_h)(p-p_h)\\
&-\mu\int_{\mathcal{T}_h} \nabla(\mathbf{u}-\mathbf{u}_h) : \nabla(\mathbf{u}_h-\mathbf{w}) + \int_{\mathcal{T}_h} (p-p_h)\,\nabla\cdot(\mathbf{u}_h-\mathbf{w})\\
&+\int_{\mathcal{E}_h^0} [(-\mu\nabla\mathbf{u}_h+p_h\mathbf{I})\mathbf{n}_e]\cdot\{\mathbf{u}-\mathbf{u}_h-\mathbf{v}_h\}\\
&+\mu\int_{\mathcal{E}_h} \frac{\sigma_e}{h_e}[\mathbf{u}_h-\mathbf{u}]\cdot[\mathbf{u}_h-\mathbf{u}+\mathbf{v}_h]\\
&+\alpha\int_{\mathcal{E}_h^0} [(\mathbf{u}_h-\mathbf{u}+\mathbf{v}_h)\cdot\mathbf{n}_e][p_h] + \mu\int_{\mathcal{E}_h} \frac{\sigma_e}{h_e}|[\mathbf{u}_h-\mathbf{u}]|^2\\
&+\mu\int_{\mathcal{E}_h} [\mathbf{u}-\mathbf{u}_h]\cdot\{\nabla(\mathbf{u}_h-\mathbf{w})\,\mathbf{n}_e\}\,.
\end{aligned} \tag{21}$$

Remark 1. In order to choose $\mathbf{w}$, we first recall that $\mathbf{u}_h = \mathbf{u}_h^{\text{cont}} + \mathbf{u}_h^{\text{disc}}$, where $\mathbf{u}_h^{\text{cont}}$ and $\mathbf{u}_h^{\text{disc}}$ denote, respectively, the continuous and discontinuous parts of $\mathbf{u}_h$. We take for $\mathbf{w}$ an approximation $S_h(\mathbf{u}_h)$ of the Scott–Zhang type (see [30]): $S_h(\mathbf{u}_h) \in [M_0^1(\mathcal{T}_h)]^d$ (recall that here $k=1$). Let $\mathcal{N}$ denote the set of vertices of $\mathcal{T}_h$, $\mathcal{N}^0$ the set of its interior vertices and $\mathcal{N}^\partial$ that of its boundary vertices. For every $\mathbf{a}$ of $\mathcal{N}^\partial$, we set

$$S_h(\mathbf{u}_h)(\mathbf{a}) = \mathbf{g}_D(\mathbf{a});$$

for every $\mathbf{a}$ of $\mathcal{N}^0$, we choose an element $E_\mathbf{a} \in \mathcal{T}_h$ with vertex $\mathbf{a}$ and set

$$S_h(\mathbf{u}_h)(\mathbf{a}) = \mathbf{u}_h^{\text{cont}}(\mathbf{a}) + \mathbf{u}_h^{\text{disc}}|_{E_\mathbf{a}};$$

then for every $\mathbf{x} \in \overline{\Omega}$, we define

$$S_h(\mathbf{u}_h)(\mathbf{x}) = \sum_{\mathbf{a}\in\mathcal{N}} \big(S_h(\mathbf{u}_h)(\mathbf{a})\big)\phi_\mathbf{a}(\mathbf{x}),$$

where, in the case of simplices $\phi_\mathbf{a}$ is the standard piecewise linear basis function, i.e., $\phi_\mathbf{a}(\mathbf{b}) = \delta_{\mathbf{a},\mathbf{b}}$ for all $\mathbf{a},\mathbf{b}$ in $\mathcal{N}$. In the case of quadrilaterals ($d=2$) or hexahedra ($d=3$), the basis function $\phi_\mathbf{a}$ is defined likewise through (4).

Remark 2. Note that, if $\mathbf{u}$ belongs to $[H^{1+s}(\Omega)]^d$ and p belongs to $H^s(\Omega)$, we can deduce from (16) that for all $\mathbf{v} \in [H_0^1(\Omega)]^d$ and $\mathbf{v}_h \in [M^k(\mathcal{T}_h) \cap H_0^1(\Omega)]^d$,

$$
\begin{aligned}
b(\mathbf{v}, p - p_h) = &-\mu \int_{\mathcal{T}_h} \nabla(\mathbf{u} - \mathbf{u}_h) : \nabla \mathbf{v} + \int_{\mathcal{T}_h} (\mathbf{f} - \mathbf{f}_h) \cdot (\mathbf{v} - \mathbf{v}_h) \\
&+ \int_{\mathcal{T}_h} (\mathbf{f}_h + \mu \Delta \mathbf{u}_h - \nabla p_h) \cdot (\mathbf{v} - \mathbf{v}_h) \\
&+ \int_{\mathcal{E}_h^0} [(-\mu \nabla \mathbf{u}_h + p_h \mathbf{I})\mathbf{n}_e] \cdot \{\mathbf{v} - \mathbf{v}_h\} - \mu \int_{\mathcal{E}_h} \{\nabla \mathbf{v}_h \mathbf{n}_e\} \cdot [\mathbf{u}_h - \mathbf{u}] .
\end{aligned} \tag{22}
$$

It is easy to check that (22) is valid for all functions $\mathbf{v}$ in $[H_0^1(\Omega)]^d$. Note that all terms involving the jump of $\mathbf{v}$ and $\mathbf{v}_h$ vanish owing that both $\mathbf{v}$ and $\mathbf{v}_h$ belong to $[H_0^1(\Omega)]^d$.

Now, we need to control $p - p_h$. To this end, we use the continuous inf-sup condition: since $p - p_h \in L_0^2(\Omega)$, there exists $\bar{\mathbf{v}} \in [H_0^1(\Omega)]^d$ such that (see [19]),

$$
\nabla \cdot \bar{\mathbf{v}} = -(p - p_h) \qquad \text{and} \qquad |\bar{\mathbf{v}}|_{[H^1(\Omega)]^d} \leq \frac{1}{\beta} \|p - p_h\|_{L^2(\Omega)} . \tag{23}
$$

Hence, using (10), it is easy to see that $\bar{\mathbf{v}} \in [H_0^1(\Omega)]^d$ satisfies:

$$
b(\bar{\mathbf{v}}, p - p_h) = \|p - p_h\|_{L^2(\Omega)}^2 . \tag{24}
$$

Then, we revert to (22) with $\bar{\mathbf{v}} \in [H_0^1(\Omega)]^d$ given by (23) and $\mathbf{v}_h = R_h(\bar{\mathbf{v}})$, where $R_h : [H_0^1(\Omega)]^d \to [M^1(\mathcal{T}_h) \cap H_0^1(\Omega)]^d$ is the standard Scott–Zhang interpolation operator (see [30]). This yields the following pressure error equality:

$$
\begin{aligned}
\|p - p_h\|_{L^2(\Omega)}^2 = &-\mu \int_{\mathcal{T}_h} \nabla(\mathbf{u} - \mathbf{u}_h) : \nabla \bar{\mathbf{v}} + \int_{\mathcal{T}_h} (\mathbf{f} - \mathbf{f}_h) \cdot (\bar{\mathbf{v}} - \mathbf{v}_h) \\
&+ \int_{\mathcal{T}_h} (\mathbf{f}_h + \mu \Delta \mathbf{u}_h - \nabla p_h) \cdot (\bar{\mathbf{v}} - \mathbf{v}_h) \\
&+ \int_{\mathcal{E}_h^0} [(-\mu \nabla \mathbf{u}_h + p_h \mathbf{I})\mathbf{n}_e] \cdot \{\bar{\mathbf{v}} - \mathbf{v}_h\} - \mu \int_{\mathcal{E}_h} \{\nabla \mathbf{v}_h \, \mathbf{n}_e\} \cdot [\mathbf{u}_h - \mathbf{u}] .
\end{aligned} \tag{25}
$$

4.2 A posteriori estimates

We first propose error indicators, based on the above error equalities; next we derive reliability and efficiency error inequalities. We start with the pressure in terms of the velocity and then derive an inequality for the velocity. All constants below are independent of h, E and e.

4.2.1 Error indicators

The error equalities (21) and (25) suggest the following error indicators:

1. the volume momentum error,

$$\eta_{m,E} := h_E \|\mathbf{f}_h + \mu\Delta\mathbf{u}_h - \nabla p_h\|_{[L^2(E)]^d}, \quad \forall E \in \mathcal{T}_h; \tag{26}$$

2. the divergence error,

$$\eta_{\mathrm{div},E} := \|\nabla\cdot\mathbf{u}_h\|_{L^2(E)}, \quad \forall E \in \mathcal{T}_h; \tag{27}$$

3. the interior penalty jump of the velocity,

$$\eta_{\mathrm{pen},\mathbf{u}} := (\frac{1}{h_e})^{\frac{1}{2}} \|[\mathbf{u}_h]\|_{[L^2(e)]^d}, \quad \forall e \in \mathcal{E}_h^0; \tag{28}$$

4. the boundary penalty error of the velocity,

$$\eta_{\mathrm{pen},D} := (\frac{1}{h_e})^{\frac{1}{2}} \|\mathbf{u}_h - \mathbf{g}_D\|_{[L^2(e)]^d}, \quad \forall e \in \mathcal{E}_h^\partial; \tag{29}$$

5. the interface jump of the momentum,

$$\eta_{m,e} := h_e^{\frac{1}{2}} \|[(-\mu\nabla\mathbf{u}_h + p_h\mathbf{I})\mathbf{n}_e]\|_{[L^2(e)]^d}, \quad \forall e \in \mathcal{E}_h^0; \tag{30}$$

6. the pressure jump,

$$\eta_{j,p} := h_e^{\frac{1}{2}} \|[p_h]\|_{L^2(e)}, \quad \forall e \in \mathcal{E}_h^0. \tag{31}$$

4.2.2 Pressure error inequality

Now, we bound the terms on the right-hand side of (25). The first four bounds below are straightforward consequences of the Cauchy-Schwarz inequality, (3), and the approximation properties of R_h [30],

$$|-\mu\int_{\mathcal{T}_h} \nabla(\mathbf{u}-\mathbf{u}_h) : \nabla\bar{\mathbf{v}}| \le \frac{\mu}{\beta}|\mathbf{u}-\mathbf{u}_h|_h \|p-p_h\|_{L^2(\Omega)}, \tag{32}$$

$$|\int_{\mathcal{T}_h} (\mathbf{f}-\mathbf{f}_h)\cdot(\bar{\mathbf{v}}-\mathbf{v}_h)| \le \frac{C}{\beta}\Big(\sum_{E\in\mathcal{T}_h} h_E^2\|\mathbf{f}-\mathbf{f}_h\|^2_{[L^2(E)]^d}\Big)^{\frac{1}{2}} \|p-p_h\|_{L^2(\Omega)}, \tag{33}$$

$$|\int_{\mathcal{T}_h} (\mathbf{f}_h+\mu\Delta\mathbf{u}_h-\nabla p_h)\cdot(\bar{\mathbf{v}}-\mathbf{v}_h)| \le \frac{C}{\beta}\Big(\sum_{E\in\mathcal{T}_h} (\eta_{m,E})^2\Big)^{\frac{1}{2}} \|p-p_h\|_{L^2(\Omega)}, \tag{34}$$

$$|\int_{\mathcal{E}_h^0}[(-\mu\nabla\mathbf{u}_h + p_h\mathbf{I})\mathbf{n}_e]\cdot\{\bar{\mathbf{v}} - \mathbf{v}_h\}| \le \frac{C}{\beta}\Big(\sum_{e\in\mathcal{E}_h^0}(\eta_{m,e})^2\Big)^{\frac{1}{2}}\|p - p_h\|_{L^2(\Omega)}. \quad (35)$$

A trace theorem in each element E is used for (35). The last term of (25) is handled by the next proposition.

Proposition 1. *There exists a constant $C > 0$, independent of h, such that for all $\mathbf{u} \in [H^1(\Omega)]^d$, $\mathbf{u}_h$, $\mathbf{v}_h$ in $[M^k(\mathcal{T}_h)]^d$,*

$$\begin{aligned}\Big|\mu\int_{\mathcal{E}_h}\{\nabla\mathbf{v}_h\,\mathbf{n}_e\}\cdot[\mathbf{u}_h - \mathbf{u}]\Big| &\le \\ &\le C\,\frac{\mu}{\beta}\Big(\sum_{e\in\mathcal{E}_h^0}(\eta_{\mathrm{pen},\mathbf{u}})^2 + \sum_{e\in\mathcal{E}_h^\partial}(\eta_{\mathrm{pen},D})^2\Big)^{\frac{1}{2}}\|p - p_h\|_{L^2(\Omega)}.\end{aligned} \quad (36)$$

Proof. Consider first the case when e belongs to $\mathcal{E}_h^0$, and let E_1 and E_2 denote the two elements of $\mathcal{T}_h$ adjacent to e. By using the regularity of the triangulation and an equivalence of norms owing that $\mathbf{v}_h$ belongs to a finite dimensional space in each E, we have

$$\begin{aligned}\Big|\int_{\mathcal{E}_h^0}\{\nabla\mathbf{v}_h\,\mathbf{n}_e\}\cdot[\mathbf{u}_h - \mathbf{u}]\Big| &\le \\ &\le C\sum_{e\in\mathcal{E}_h^0}\big(\frac{1}{h_e}\big)^{\frac{1}{2}}\|[\mathbf{u} - \mathbf{u}_h]\|_{[L^2(e)]^d}\Big(|\mathbf{v}_h|_{[H^1(E_1)]^d} + |\mathbf{v}_h|_{[H^1(E_2)]^d}\Big).\end{aligned}$$

Any element E of $\mathcal{T}_h$ occurs in this inequality at most $d+1$ times in the case of simplices and $2d$ times in the case of quadrilaterals ($d = 2$) or hexahedra ($d = 3$). Analogously, if e belongs to $\mathcal{E}_h^\partial$, we obtain

$$\Big|\int_{\mathcal{E}_h^\partial}\{\nabla\mathbf{v}_h\,\mathbf{n}_e\}\cdot[\mathbf{u}_h - \mathbf{u}]\Big| \le C\sum_{e\in\mathcal{E}_h^\partial}\big(\frac{1}{h_e}\big)^{\frac{1}{2}}\|[\mathbf{u} - \mathbf{u}_h]\|_{[L^2(e)]^d}|\mathbf{v}_h|_{[H^1(E)]^d}\,,$$

where E is the element in $\mathcal{T}_h$ that has e as an edge ($d = 2$) or face ($d = 3$). This, (3), and the stability of R_h lead readily to (36). □

By substituting (32)–(36) into (25), we immediately derive a first pressure error inequality,

$$\begin{aligned}\|p-p_h\|_{L^2(\Omega)} \le\ & \frac{\mu}{\beta}|\mathbf{u}-\mathbf{u}_h|_h + \frac{C}{\beta}\Big[\Big(\sum_{E\in\mathcal{T}_h} h_E^2\|\mathbf{f}-\mathbf{f}_h\|^2_{[L^2(E)]^d}\Big)^{\frac12} \\ & +\Big(\sum_{E\in\mathcal{T}_h}(\eta_{m,E})^2\Big)^{\frac12} + \Big(\sum_{e\in\mathcal{E}_h^0}(\eta_{m,e})^2\Big)^{\frac12} \\ & +\mu\Big(\sum_{e\in\mathcal{E}_h^0}(\eta_{\mathrm{pen},\mathbf{u}})^2 + \sum_{e\in\mathcal{E}_h^\partial}(\eta_{\mathrm{pen},D})^2\Big)^{\frac12}\Big].\end{aligned} \tag{37}$$

To simplify, set temporarily

$$\begin{aligned}\eta_{\mathbf{f},m} :=&\Big(\sum_{E\in\mathcal{T}_h} h_E^2\|\mathbf{f}-\mathbf{f}_h\|^2_{[L^2(E)]^d}\Big)^{\frac12} + \Big(\sum_{E\in\mathcal{T}_h}(\eta_{m,E})^2\Big)^{\frac12} + \Big(\sum_{e\in\mathcal{E}_h^0}(\eta_{m,e})^2\Big)^{\frac12}, \\ \eta_{\mathrm{pen}} :=&\Big(\sum_{e\in\mathcal{E}_h^0}(\eta_{\mathrm{pen},\mathbf{u}})^2 + \sum_{e\in\mathcal{E}_h^\partial}(\eta_{\mathrm{pen},D})^2\Big)^{\frac12}.\end{aligned} \tag{38}$$

Then (37) becomes

$$\|p-p_h\|_{L^2(\Omega)} \le \frac{\mu}{\beta}|\mathbf{u}-\mathbf{u}_h|_h + \frac{C}{\beta}\big(\eta_{\mathbf{f},m} + \mu\,\eta_{\mathrm{pen}}\big). \tag{39}$$

4.2.3 Velocity error inequality

We now bound the terms on the right-hand side of (21); recall that here, $\mathbf{v}_h$ is given by (20). Let us begin with the terms not involving $\mathbf{w}$,

$$|\int_{\mathcal{T}_h}(\mathbf{f}-\mathbf{f}_h)\cdot(\mathbf{u}-\mathbf{u}_h-\mathbf{v}_h)| \le C\Big(\sum_{E\in\mathcal{T}_h} h_E^2\,\|\mathbf{f}-\mathbf{f}_h\|^2_{[L^2(E)]^d}\Big)^{\frac12}|\mathbf{u}-\mathbf{u}_h|_h; \tag{40}$$

$$|\int_{\mathcal{T}_h}(\mathbf{f}_h+\mu\Delta\mathbf{u}_h-\nabla p_h)\cdot(\mathbf{u}-\mathbf{u}_h-\mathbf{v}_h)| \le C\Big(\sum_{E\in\mathcal{T}_h}\big(\eta_{m,E}\big)^2\Big)^{\frac12}|\mathbf{u}-\mathbf{u}_h|_h; \tag{41}$$

$$|-\int_{\mathcal{T}_h}(\nabla\cdot\mathbf{u}_h)(p-p_h)| \le \Big(\sum_{E\in\mathcal{T}_h}\big(\eta_{\mathrm{div},E}\big)^2\Big)^{\frac12}\|p-p_h\|_{L^2(\Omega)}; \tag{42}$$

$$|\int_{\mathcal{E}_h^0}[(-\mu\nabla\mathbf{u}_h+p_h\mathbf{I})\mathbf{n}_e]\cdot\{\mathbf{u}-\mathbf{u}_h-\mathbf{v}_h\}| \le C\Big(\sum_{e\in\mathcal{E}_h^0}\big(\eta_{m,e}\big)^2\Big)^{\frac12}|\mathbf{u}-\mathbf{u}_h|_h; \tag{43}$$

$$
\begin{aligned}
&|\mu \int_{\mathcal{E}_h} \frac{\sigma_e}{h_e}\,[\mathbf{u}_h - \mathbf{u}]\cdot[\mathbf{u}_h - \mathbf{u} + \mathbf{v}_h]| \le \\
&\quad \le C\mu\,(\max \sigma_e)\Big(\sum_{e\in\mathcal{E}_h^0}\big(\eta_{\mathrm{pen},\mathbf{u}}\big)^2 + \sum_{e\in\mathcal{E}_h^\partial}\big(\eta_{\mathrm{pen},D}\big)^2\Big)^{\frac12}\,|\mathbf{u}-\mathbf{u}_h|_h,
\end{aligned}
\tag{44}
$$

where the maximum of σ_e is taken over all e in $\mathcal{E}_h$;

$$
|\alpha \int_{\mathcal{E}_h^0} [(\mathbf{u}_h - \mathbf{u} + \mathbf{v}_h)\cdot\mathbf{n}_e][p_h]| \le \alpha\, C\Big(\sum_{e\in\mathcal{E}_h^0}\big(\eta_{j,p}\big)^2\Big)^{\frac12}\,|\mathbf{u}-\mathbf{u}_h|_h. \tag{45}
$$

To estimate the three terms involving $\mathbf{w}$, we employ the following approximation property of S_h, a simple variant of the property established for example in [8, 18, 23].

Proposition 2. *There exists a constant $C > 0$, independent of h and $\mathbf{u}_h$, such that*

$$
|S_h(\mathbf{u}_h) - \mathbf{u}_h|_h \le C\Big(\sum_{e\in\mathcal{E}_h^0}\frac{1}{h_e}\|[\mathbf{u}_h]\|^2_{L^2(e)} + \sum_{e\in\mathcal{E}_h^\partial}\frac{1}{h_e}\|\mathbf{u}_h - \mathbf{g}_D\|^2_{L^2(e)}\Big)^{\frac12}. \tag{46}
$$

As usual, (46) is first derived locally in each element and next summed over all elements. Note that it involves interior and boundary terms. By applying it locally, we obtain,

$$
|-\mu \int_{\mathcal{T}_h} \nabla(\mathbf{u}-\mathbf{u}_h) : \nabla(\mathbf{u}_h - \mathbf{w})| \le \mu\, C\,\eta_{\mathrm{pen}}\,|\mathbf{u}-\mathbf{u}_h|_h; \tag{47}
$$

$$
|\int_{\mathcal{T}_h} (p-p_h)\,\nabla\cdot(\mathbf{u}_h - \mathbf{w})| \le C\,\eta_{\mathrm{pen}}\,\|p-p_h\|_{L^2(\Omega)}, \tag{48}
$$

Finally, the term on $\mathcal{E}_h$ is treated by combining locally an equivalence of norms as in (36) with (46),

$$
|\mu \int_{\mathcal{E}_h} [\mathbf{u}-\mathbf{u}_h]\cdot(\{\nabla(\mathbf{u}_h - \mathbf{w})\}\,\mathbf{n}_e)| \le \mu\, C\,\big(\eta_{\mathrm{pen}}\big)^2. \tag{49}
$$

By substituting (40)–(45), (47)–(49) into (21), and cancelling the jump term on both sides, we obtain a first preliminary inequality,

$$\begin{aligned}\mu\,|\mathbf{u}-\mathbf{u}_h|_h^2 \le C\Big[\Big(\sum_{E\in\mathcal{T}_h} h_E^2\,\|\mathbf{f}-\mathbf{f}_h\|^2_{[L^2(E)]^d}\Big)^{\frac{1}{2}} + \Big(\sum_{E\in\mathcal{T}_h}\big(\eta_{m,E}\big)^2\Big)^{\frac{1}{2}}\\
+\Big(\sum_{e\in\mathcal{E}_h^0}\big(\eta_{m,e}\big)^2\Big)^{\frac{1}{2}} + \mu(1+\max\sigma_e)\eta_{\text{pen}} + \alpha\Big(\sum_{e\in\mathcal{E}_h^0}\big(\eta_{j,p}\big)^2\Big)^{\frac{1}{2}}\Big]\,|\mathbf{u}-\mathbf{u}_h|_h\\
+\Big[\Big(\sum_{E\in\mathcal{T}_h}\big(\eta_{\text{div},E}\big)^2\Big)^{\frac{1}{2}} + C\,\eta_{\text{pen}}\Big]\|p-p_h\|_{L^2(\Omega)} + C\,\mu\big(\eta_{\text{pen}}\big)^2,\end{aligned} \tag{50}$$

where the maximum of σ_e is taken over all e of $\mathcal{E}_h$. With the simplified notation (38), (50) reads

$$\begin{aligned}\mu\,|\mathbf{u}-\mathbf{u}_h|_h^2 \le \|p-p_h\|_{L^2(\Omega)}\Big[\Big(\sum_{E\in\mathcal{T}_h}\big(\eta_{\text{div},E}\big)^2\Big)^{\frac{1}{2}} + C\,\eta_{\text{pen}}\Big] + C\,\mu\big(\eta_{\text{pen}}\big)^2\\
+C\Big[\eta_{\mathbf{f},m} + \mu(1+\max\sigma_e)\eta_{\text{pen}} + \alpha\Big(\sum_{e\in\mathcal{E}_h^0}\big(\eta_{j,p}\big)^2\Big)^{\frac{1}{2}}\Big]\,|\mathbf{u}-\mathbf{u}_h|_h.\end{aligned} \tag{51}$$

By substituting (39) into (51) and collecting terms, we obtain a second preliminary inequality

$$\begin{aligned}\mu\,|\mathbf{u}-\mathbf{u}_h|_h^2 \le |\mathbf{u}-\mathbf{u}_h|_h\Big[\frac{\mu}{\beta}\Big(\sum_{E\in\mathcal{T}_h}\big(\eta_{\text{div},E}\big)^2\Big)^{\frac{1}{2}}\\
+C\Big(\mu\,\eta_{\text{pen}}\big(\frac{1}{\beta}+1+\max\sigma_e\big) + \eta_{\mathbf{f},m} + \alpha\Big(\sum_{e\in\mathcal{E}_h^0}\big(\eta_{j,p}\big)^2\Big)^{\frac{1}{2}}\Big)\Big]\\
+C\,\mu\,\big(\eta_{\text{pen}}\big)^2 + \frac{C}{\beta}\big(\eta_{\mathbf{f},m}+\mu\,\eta_{\text{pen}}\big)\Big(\Big(\sum_{E\in\mathcal{T}_h}\big(\eta_{\text{div},E}\big)^2\Big)^{\frac{1}{2}} + C\,\eta_{\text{pen}}\Big).\end{aligned}$$

The term $|\mathbf{u}-\mathbf{u}_h|_h$ on the right-hand side is eliminated by Young's inequality,

$$\begin{aligned}\frac{\mu}{2}\,|\mathbf{u}-\mathbf{u}_h|_h^2 \le \frac{1}{2\mu}\Big[\frac{\mu}{\beta}\Big(\sum_{E\in\mathcal{T}_h}\big(\eta_{\text{div},E}\big)^2\Big)^{\frac{1}{2}}\\
+C\Big(\mu\,\eta_{\text{pen}}\big(\frac{1}{\beta}+1+\max\sigma_e\big) + \eta_{\mathbf{f},m} + \alpha\Big(\sum_{e\in\mathcal{E}_h^0}\big(\eta_{j,p}\big)^2\Big)^{\frac{1}{2}}\Big)\Big]^2\\
+C\,\mu\,\big(\eta_{\text{pen}}\big)^2 + \frac{C}{\beta}\big(\eta_{\mathbf{f},m}+\mu\,\eta_{\text{pen}}\big)\Big(\Big(\sum_{E\in\mathcal{T}_h}\big(\eta_{\text{div},E}\big)^2\Big)^{\frac{1}{2}} + C\,\eta_{\text{pen}}\Big)\end{aligned}$$

By expanding the square and applying Young's inequality to the remaining terms, we infer

$$\begin{aligned}\frac{\mu}{2}\,|\mathbf{u}-\mathbf{u}_h|_h^2 \le \frac{1}{2\mu}\Big[\frac{4\mu^2}{\beta^2}\sum_{E\in\mathcal{T}_h}\big(\eta_{\mathrm{div},E}\big)^2 + 4C^2\mu^2\eta_{\mathrm{pen}}^2\big(\frac{1}{\beta}+1+\max\sigma_e\big)^2\\ +4\,C^2\eta_{\mathbf{f},m}^2 + 4C^2\alpha^2\sum_{e\in\mathcal{E}_h^0}\big(\eta_{j,p}\big)^2\Big]\\ +C\mu\,\eta_{\mathrm{pen}}^2 + C^2\big(\eta_{\mathbf{f},m}^2+\mu^2\,\eta_{\mathrm{pen}}^2\big) + \frac{1}{\beta^2}\sum_{E\in\mathcal{T}_h}\big(\eta_{\mathrm{div},E}\big)^2 + \frac{C^2}{\beta^2}\eta_{\mathrm{pen}}^2.\end{aligned}$$

By grouping these terms and merging all unspecified constants into a single one, we derive

$$\begin{aligned}\frac{\mu}{2}\,|\mathbf{u}-\mathbf{u}_h|_h^2 \le \frac{1}{\beta^2}(1+2\,\mu)\sum_{E\in\mathcal{T}_h}\big(\eta_{\mathrm{div},E}\big)^2\\ +C\Big(\big(\mu\big(2(\frac{1}{\beta}+1{+}\max\sigma_e\big)^2+1+\mu\big)+\frac{1}{\beta^2}\big)\eta_{\mathrm{pen}}^2\\ +(1+\frac{2}{\mu})\eta_{\mathbf{f},m}^2 + 2\frac{\alpha^2}{\mu}\sum_{e\in\mathcal{E}_h^0}\big(\eta_{j,p}\big)^2\Big).\end{aligned} \tag{52}$$

Finally, by expanding the notation (38), we obtain a first reliability error bound for the velocity,

$$\begin{aligned}\mu\,|\mathbf{u}-\mathbf{u}_h|_h^2 \le \frac{4\mu+2}{\beta^2}\sum_{E\in\mathcal{T}_h}\big(\eta_{\mathrm{div},E}\big)^2 + C\Big(\frac{4\alpha^2}{\mu}\sum_{e\in\mathcal{E}_h^0}\big(\eta_{j,p}\big)^2\\ +2\,\big(\mu\big(2(\frac{1}{\beta}+1+\max\sigma_e\big)^2+1+\mu\big)+\frac{1}{\beta^2}\big)\Big(\sum_{e\in\mathcal{E}_h^0}\big(\eta_{\mathrm{pen},\mathbf{u}}\big)^2+\sum_{e\in\mathcal{E}_h^\partial}\big(\eta_{\mathrm{pen},D}\big)^2\Big)\\ +\big(\frac{4}{\mu}+2\big)\Big(\sum_{E\in\mathcal{T}_h}h_E^2\,\|\mathbf{f}-\mathbf{f}_h\|_{[L^2(E)]^d}^2 + \sum_{E\in\mathcal{T}_h}\big(\eta_{m,E}\big)^2+\sum_{e\in\mathcal{E}_h^0}\big(\eta_{m,e}\big)^2\Big)\Big).\end{aligned} \tag{53}$$

A reliability bound for the pressure follows immediately by combining (53) with (37).

Of course,

$$\mu\Big(\int_{\mathcal{E}_h}\frac{\sigma_e}{h_e}|[\mathbf{u}-\mathbf{u}_h]|^2\Big)^{\frac12} \le \mu(\max\sigma_e)^{\frac12}\Big[\sum_{e\in\mathcal{E}_h^0}\big(\eta_{\mathrm{pen},\mathbf{u}}\big)^2+\sum_{e\in\mathcal{E}_h^\partial}\big(\eta_{\mathrm{pen},D}\big)^2\Big]^{\frac12}. \tag{54}$$

4.2.4 Local Error indicator

For each $E\in\mathcal{T}_h$, we define the local error indicator:

$$\eta_E^2 := \eta_{m,E}^2+\eta_{\mathrm{div},E}^2+\frac{1}{2}\sum_{e\in\mathcal{E}(E)\cap\mathcal{E}_h^0}(\eta_{\mathrm{pen},\mathbf{u}}^2+\eta_{m,e}^2+\eta_{j,p}^2)+\sum_{e\in\mathcal{E}(E)\cap\mathcal{E}_h^\partial}\eta_{\mathrm{pen},D}^2\,, \tag{55}$$

where $\mathcal{E}(E)$ denotes the set of edges ($d = 2$) or faces ($d = 3$) of the element E; we remark that the coefficient $1/2$ in equation (55) is introduced because each interior edge or face occurs twice. From the analysis in previous sections, we have the following result:

Theorem 1. *Let the exact solution* $(\mathbf{u}, p)$ *of* (2) *belong to* $[H^{1+s}(\Omega)]^d \times H^s(\Omega)$ *for some real number* $s > 0$*. Assume that the triangulation* $\mathcal{T}_h$ *is regular and the penalty parameters* $\sigma_e > 0$ *are independent of* h*. For the values* $k = 1$*,* $\epsilon = -1$*, and* $\alpha = \pm\frac{1}{2}$*, let* $(\mathbf{u}_h, p_h)$ *solve* (8)*. There exists a positive constant* C*, independent of* h*, such that*

$$\mu \|\mathbf{u} - \mathbf{u}_h\|_{EG}^2 \leq C \sum_{E \in \mathcal{T}_h} \left(h_E^2 \|\mathbf{f} - \mathbf{f}_h\|_{[L^2(E)]^d}^2 + \eta_E^2 \right), \tag{56}$$

and

$$\|p - p_h\|_{L^2(\Omega)}^2 \leq C \sum_{E \in \mathcal{T}_h} \left(h_E^2 \|\mathbf{f} - \mathbf{f}_h\|_{[L^2(E)]^d}^2 + \eta_E^2 \right). \tag{57}$$

Proof. Inequality (56) is a consequence of inequalities (53) and (54). Inequality (57) is deduced from inequalities (37) and (56). □

From the previous result, η_E can be used as a reliable error indicator to measure the error in the velocity and in the pressure.

Remark 3. Following the same steps in the NIPG method ($\epsilon = 1$), we arrive at the same bounds. For the IIPG method ($\epsilon = 0$), the calculations are slightly simpler, but lead also to the same error indicator. Thus, the error indicator η_E can be used in combination with the NIPG and IIPG variants of the enriched Galerkin method too.

Remark 4. Neither the discrete inf-sup condition (13) nor the particular choice of penalty parameters σ_e have been used explicitly in proving (56) and (57). However, they are used in Theorem 1 to derive existence of the discrete solution.

4.2.5 Efficiency

In this subsection, we study the efficiency of the error indicator η_E for the Symmetric Interior Penalty enriched Galerkin method. All constants C below are independent of h, E, and e. We proceed in five steps.

1) First, since $\nabla \cdot \mathbf{u} = 0$ in Ω, we immediately have that

$$\eta_{\mathrm{div},E} = \|\nabla \cdot \mathbf{u}_h\|_{L^2(E)} = \|\nabla \cdot (\mathbf{u} - \mathbf{u}_h)\|_{L^2(E)} \leq d^{\frac{1}{2}} |\mathbf{u} - \mathbf{u}_h|_{[H^1(E)]^d}. \tag{58}$$

2) Obviously, by definition,

$$\eta_{\mathrm{pen},\mathbf{u}} = \frac{1}{\sigma_e^{\frac{1}{2}}} \Big(\frac{\sigma_e}{h_e}\Big)^{\frac{1}{2}} \|[\mathbf{u}_h]\|_{[L^2(e)]^d},$$
$$\eta_{\mathrm{pen},D} = \frac{1}{\sigma_e^{\frac{1}{2}}} \Big(\frac{\sigma_e}{h_e}\Big)^{\frac{1}{2}} \|[\mathbf{u}_h - \mathbf{g}_D]\|_{[L^2(e)]^d}; \tag{59}$$

this bounds trivially the penalty jumps of the velocity.

For the remaining steps, we use the localisation technique introduced by Verfürth (see, for instance, [33]).

3) For any element E of $\mathcal{T}_h$, let b_E be the usual element-bubble function (see [33]). We first take

$$\mathbf{v} = \boldsymbol{\psi}_E := b_E\,(\mathbf{f}_h + \mu\,\Delta\mathbf{u}_h - \nabla p_h),$$

and $\mathbf{v}_h = \mathbf{0}$ in (16). Since $\boldsymbol{\psi}_E = \mathbf{0}$ on the boundary of E, (16) reduces to:

$$\mu\, a_{-1}(\mathbf{u}-\mathbf{u}_h, \boldsymbol{\psi}_E) + b(\boldsymbol{\psi}_E, p - p_h) = \int_E (\mathbf{f} - \mathbf{f}_h)\cdot\boldsymbol{\psi}_E$$
$$+ \int_E (\mathbf{f}_h + \mu\,\Delta\mathbf{u}_h - \nabla p_h)\cdot\boldsymbol{\psi}_E$$
$$+\mu \int_{\mathcal{E}_h^0\cap\partial E} [\mathbf{u}_h]\cdot\{\nabla\boldsymbol{\psi}_E\mathbf{n}_e\} + \mu \int_{\mathcal{E}_h^\partial\cap\partial E} (\nabla\boldsymbol{\psi}_E\,\mathbf{n})\cdot(\mathbf{u}_h - \mathbf{g}_D)\,.$$

Therefore, by expanding the two bilinear forms, passing the expression of interest to the left-hand side, and cancelling some terms, this leads to

$$\int_E (\mathbf{f}_h + \mu\,\Delta\mathbf{u}_h - \nabla p_h)\cdot\boldsymbol{\psi}_E = \mu \int_E \nabla(\mathbf{u}-\mathbf{u}_h) : \nabla\boldsymbol{\psi}_E$$
$$- \int_E (p - p_h)\nabla\cdot\boldsymbol{\psi}_E - \int_E (\mathbf{f}-\mathbf{f}_h)\cdot\boldsymbol{\psi}_E\,. \tag{60}$$

Since $\mathbf{f}_h + \mu\,\Delta\mathbf{u}_h - \nabla p_h$ belongs to a finite dimensional space in E, a local equivalence of norms yields

$$\int_E (\mathbf{f}_h + \mu\,\Delta\mathbf{u}_h - \nabla p_h)\cdot\boldsymbol{\psi}_E \;\geq\; C\,\|\mathbf{f}_h + \mu\,\Delta\mathbf{u}_h - \nabla p_h\|^2_{[L^2(E)]^d}\,, \tag{61}$$

and by a local inverse inequality,

$$\|\nabla\boldsymbol{\psi}_E\|_{[L^2(E)]^{d\times d}} \;\leq\; C\,h_E^{-1}\,\|\mathbf{f}_h + \mu\,\Delta\mathbf{u}_h - \nabla p_h\|_{[L^2(E)]^d}\,. \tag{62}$$

Of course,

$$\|\boldsymbol{\psi}_E\|_{[L^2(E)]^d} \;\leq\; \|\mathbf{f}_h + \mu\,\Delta\mathbf{u}_h - \nabla p_h\|_{[L^2(E)]^d}\,. \tag{63}$$

Therefore, by applying the Cauchy-Schwarz inequality on the right-hand side of (60), using (61), (62) and (63), cancelling the common factor on both sides and multiplying both sides by h_E, we obtain that

$$\eta_{m,E} \leq C\Big(\mu\,|\mathbf{u}-\mathbf{u}_h|_{[H^1(E)]^d} + \|p-p_h\|_{L^2(E)} + h_E\,\|\mathbf{f}-\mathbf{f}_h\|_{[L^2(E)]^d}\Big). \qquad (64)$$

4) Now we consider the interface jump of the momentum, $\eta_{m,e}$. Let e be an interior edge or face shared by two elements, E_1 and E_2 and let $\omega_e = E_1 \cup E_2$. Let b_e be the usual edge or face bubble function (see [33]), and denote

$$\boldsymbol{\rho}_e = b_e[(-\mu\nabla\mathbf{u}_h + p_h\mathbf{I})\mathbf{n}_e].$$

We consider $\boldsymbol{\psi}_e = L(\boldsymbol{\rho}_e)$, where L is an appropriate lifting operator from $H^{1/2}_{00}(e)$ into $H^1_0(\omega_e)$. As usual, L is first constructed on two adjacent reference elements $\widehat{\omega_e}$ and then passed to ω_e by a continuous, locally affine transformation in the case of simplices. On quadrilateral ($d=2$) or hexahedral elements ($d=3$), the affine transformation is replaced by the inverse of a locally bilinear or trilinear transformation, according to the dimension, so that

$$\forall f \in H^{1/2}_{00}(e), \quad |L(f)|_{H^1(\omega_e)} \leq C|f|_{H^{1/2}_{00}(e)}, \qquad (65)$$

with a constant C independent of h, e, ω_e. Therefore, by Poincaré's inequality,

$$\begin{aligned} \|L(\boldsymbol{\rho}_e)\|_{[L^2(\omega_e)]^d} &\leq C\,h_e|L(\boldsymbol{\rho}_e)|_{[H^1(\omega_e)]^d} \\ &\leq C\,h_e|\boldsymbol{\rho}_e|_{[H^{1/2}_{00}(e)]^d} \leq C\,h_e^{\frac{1}{2}}\,\|\boldsymbol{\rho}_e\|_{[L^2(e)]^d}, \end{aligned} \qquad (66)$$

by a local inverse inequality valid in finite-dimensional spaces on $\hat{e}$. Similarly,

$$h_e^{\frac{1}{2}}\,|L(\boldsymbol{\rho}_e)|_{[H^1(\omega_e)]^d} \leq C\,\|\boldsymbol{\rho}_e\|_{[L^2(e)]^d}. \qquad (67)$$

On the one hand, we have by equivalence of norms in finite dimensional spaces on $\hat{e}$,

$$\int_e [(-\mu\nabla\mathbf{u}_h + p_h\mathbf{I})\mathbf{n}_e]\cdot\boldsymbol{\rho}_e \geq C\|[(-\mu\nabla\mathbf{u}_h + p_h\mathbf{I})\mathbf{n}_e]\|^2_{[L^2(e)]^d}. \qquad (68)$$

On the other hand, by testing (16) with $\mathbf{v} = L(\boldsymbol{\rho}_e)$ and $\mathbf{v}_h = \mathbf{0}$, and taking into account that $L(\boldsymbol{\rho}_e)$ does not jump, we obtain

$$\begin{aligned} \int_e [(-\mu\nabla\mathbf{u}_h + p_h\mathbf{I})\mathbf{n}_e]\cdot\boldsymbol{\rho}_e &= \mu\int_{\omega_e}\nabla(\mathbf{u}-\mathbf{u}_h):\nabla L(\boldsymbol{\rho}_e) - \int_{\omega_e}(p-p_h)\nabla\cdot L(\boldsymbol{\rho}_e) \\ &- \int_{\omega_e}(\mathbf{f}-\mathbf{f}_h)\cdot L(\boldsymbol{\rho}_e) - \int_{\omega_e}(\mathbf{f}_h + \mu\Delta\mathbf{u}_h - \nabla p_h)\cdot L(\boldsymbol{\rho}_e), \end{aligned}$$

where it is understood that the integrals over ω_e are taken element by element. Finally, (68), (66), and (67) yield,

$$\begin{aligned}\eta_{m,e} &\le C\Big(\mu\|\nabla(\mathbf{u}-\mathbf{u}_h)\|_{[L^2(\omega_e)]^{d\times d}} + \|p-p_h\|_{L^2(\omega_e)} \\ &+ h_e\,\|\mathbf{f}-\mathbf{f}_h\|_{[L^2(\omega_e)]^d} + h_e\,\|\mathbf{f}_h+\mu\Delta\mathbf{u}_h-\nabla p_h\|_{[L^2(\omega_e)]^d}\Big),\end{aligned}$$

which together with (64) and the regularity of the triangulation gives the bound,

$$\begin{aligned}\eta_{m,e} \le C\Big(&\mu\|\nabla(\mathbf{u}-\mathbf{u}_h)\|_{[L^2(\omega_e)]^{d\times d}} + \|p-p_h\|_{L^2(\omega_e)} \\ &+\Big(\sum_{E\in\omega_e} h_E^2\|\mathbf{f}-\mathbf{f}_h\|^2_{[L^2(E)]^d}\Big)^{\frac12} + \Big(\sum_{E\in\omega_e}\big(\eta_{m,E}\big)^2\Big)^{\frac12}\Big).\end{aligned} \tag{69}$$

5) Finally, to bound the pressure jump $\eta_{j,p}$ from above, we consider an interpolation operator of the Scott–Zhang type, see for example [17] $T_h : L^2_0(\Omega) \to M^1_0(\mathcal{T}_h)$ so that $T_h(p)$ does not jump. We consider again an interior edge or face $e \in \mathcal{E}^0_h$, shared by two elements E_1 and E_2, and denote $\omega_e = E_1 \cup E_2$. Then,

$$\begin{aligned}\eta_{j,p} &= h_e^{\frac12}\,\|[T_h(p)-p_h]\|_{L^2(e)} \\ &= h_e^{\frac12}\,\|(T_h(p)-p_h)|_{E_1} - (T_h(p)-p_h)|_{E_2}\|_{L^2(e)} \\ &\le C\,\|T_h(p)-p_h\|_{L^2(\omega_e)} \\ &\le C\,\|T_h(p)-p\|_{L^2(\omega_e)} + C\,\|p-p_h\|_{L^2(\omega_e)},\end{aligned} \tag{70}$$

again by an equivalence of norms in finite dimensions in $\widehat{\omega_e}$.

By collecting inequalities (64), (58), (59), (69), and (70), we obtain the desired efficiency bound.

Theorem 2. *Under the assumptions of Theorem 1, there exists a positive constant C, independent of h, E and e, such that*

$$\begin{aligned}\eta_E^2 &\le C\Big(\|\mathbf{u}-\mathbf{u}_h\|^2_{EG,\omega(E)} + \|p-p_h\|^2_{L^2(\omega(E))} \\ &+ \|T_h(p)-p\|^2_{L^2(\omega(E))} + h_E^2\|\mathbf{f}-\mathbf{f}_h\|^2_{[L^2(\omega(E))]^d}\Big)\end{aligned}$$

where $\omega(E) = \cup\{E' \in \mathcal{T}_h : E'$ shares at least an edge (face) with $E\}$.

5 Numerical results

We implemented the adaptive algorithm based on the a posteriori error indicator η_E defined in (55) in a parallel code in FreeFem++ [20] and tested it over the following example. We consider the L-shaped domain $\Omega = [-1,1]^2 \setminus ([0,1]\times[-1,0])$ with the data $\mu = 1$, $\mathbf{f} = \mathbf{0}$ and

$$\mathbf{g}_D = \begin{cases} (4y(1-y),0)^{\mathtt{t}} & \text{if } x = 1\,, \\ (0,-4x(x+1))^{\mathtt{t}} & \text{if } y = -1\,, \\ \mathbf{0} & \text{otherwise}\,. \end{cases}$$

Note that $\mathbf{g}_D$ satisfies (1), $\int_\Gamma \mathbf{g}_D \cdot \mathbf{n} = 0$. The choice of parameters is $\sigma_e = 8$, $\forall\, e \in \mathcal{E}_h$, and $\alpha = 0.5$. Since the exact solution is not known, the performance of our method is evaluated by comparing its output with the discrete solution obtained using the Hood-Taylor element over a very fine mesh with 160 075 triangles and 723 643 degrees of freedom (DOF).

We start the adaptive algorithm on a coarse mesh with 84 triangles. In every adaptive step, we rebuild the mesh and control its shape-regularity by bounding the gradient of the mesh size function; for more details, see [7]. Figure 3 depicts the graph of the total error versus the DOF for the SIPG, NIPG and IIPG versions of the enriched Galerkin method. We observe that the adaptive algorithm converges faster than the one based on uniform refinement. Figures 4 and 5 present, respectively, the graph of the velocity EG error and the pressure L^2-error versus the DOF for the SIPG, NIPG and IIPG versions of the enriched Galerkin method. Although they are not presented here, we tested some individual error indicators and found that in the example considered here, the boundary penalty error on the velocity (29) was the dominant contribution to the total error η. For instance, the divergence error (27) was negligible. Figure 6 shows the graph of the global indicator η, $\eta^2 := \sum_{E\in\mathcal{T}_h} \eta_E^2$, versus the DOF for the SIPG, NIPG and IIPG versions of the enriched Galerkin method. In Figures 3-6, the (green) dashed line indicates the theoretical order of convergence.

We define the efficiency index as the ratio of the global indicator η to the total error. In Figure 7 we can see the efficiency index versus the DOF for the SIPG, NIPG and IIPG versions of the enriched Galerkin method. The efficiency indices for the algorithms based on adaptive refinement tend to the value 3.6 in all cases. They are somewhat larger than in the case of a uniform mesh because the adaptive algorithm produces a highly distorted mesh, see Figure 8.

Finally, Figure 8 depicts the initial mesh and the mesh obtained after 9 iterations with the adaptive SIP-EG method. We observe that the refinement is highly concentrated around the origin.

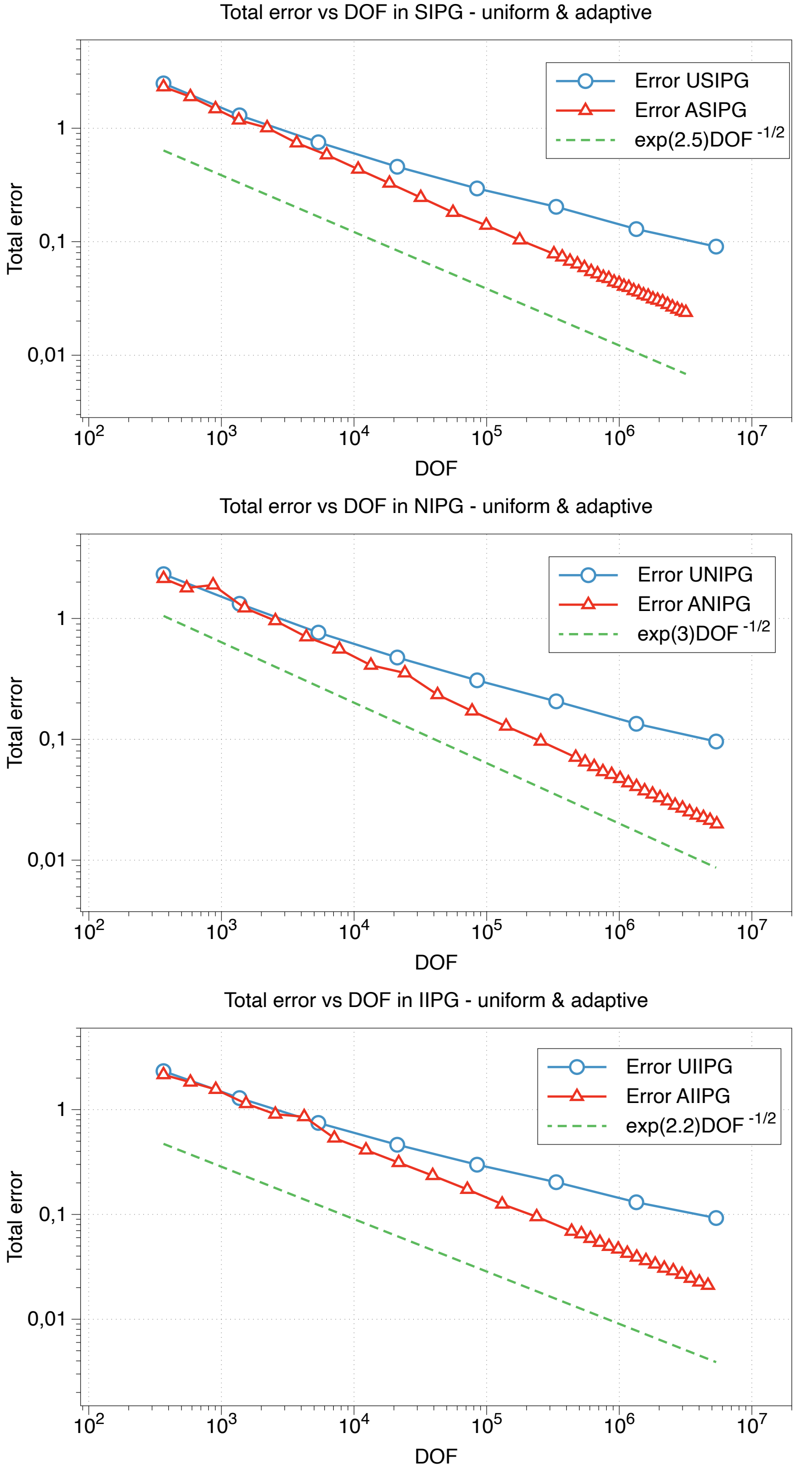

Fig. 3: Total error vs. DOF for SIPG (up), NIPG (center) and IIPG (bottom).

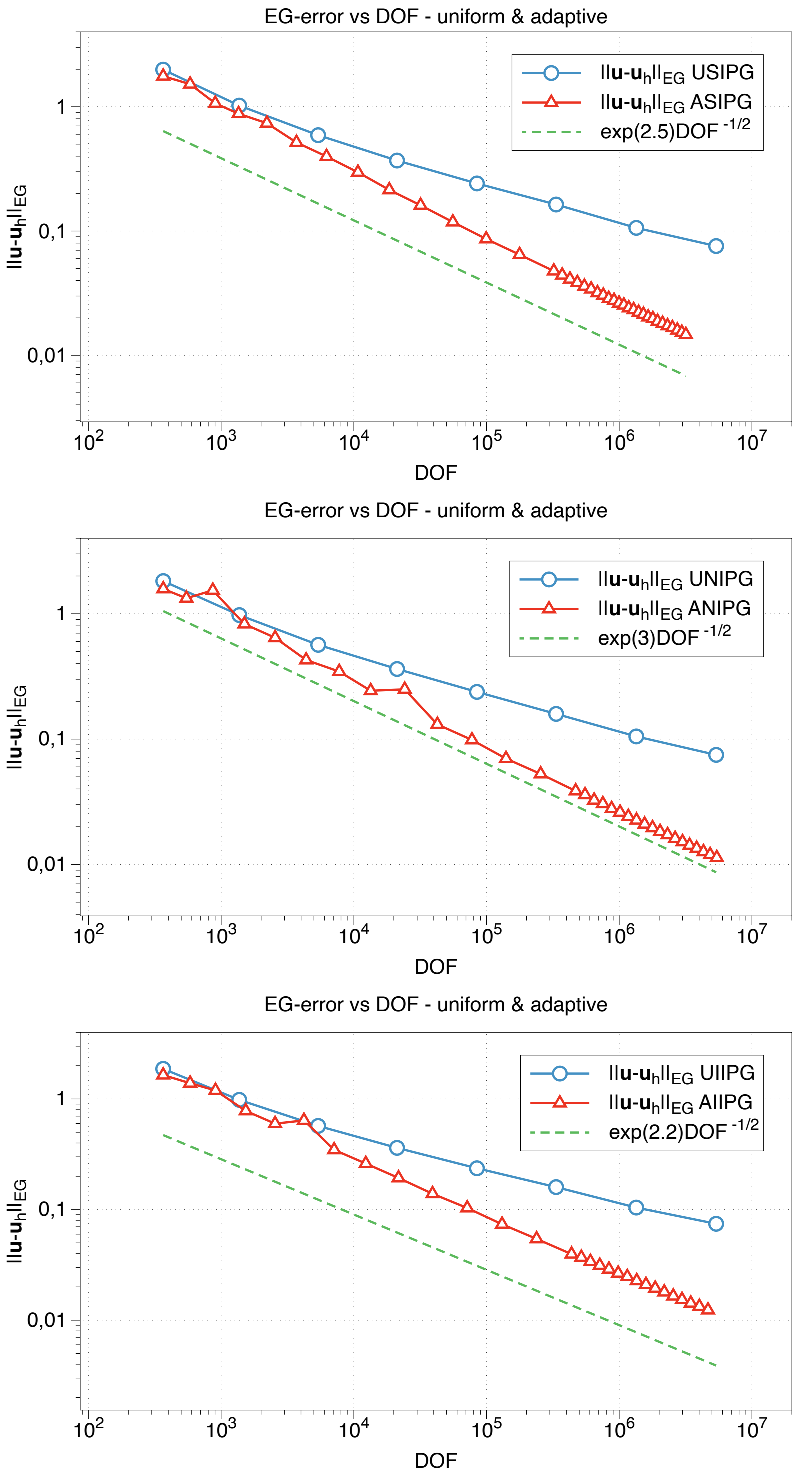

Fig. 4: Velocity EG error vs. DOF for SIPG (up), NIPG (center) and IIPG (bottom).

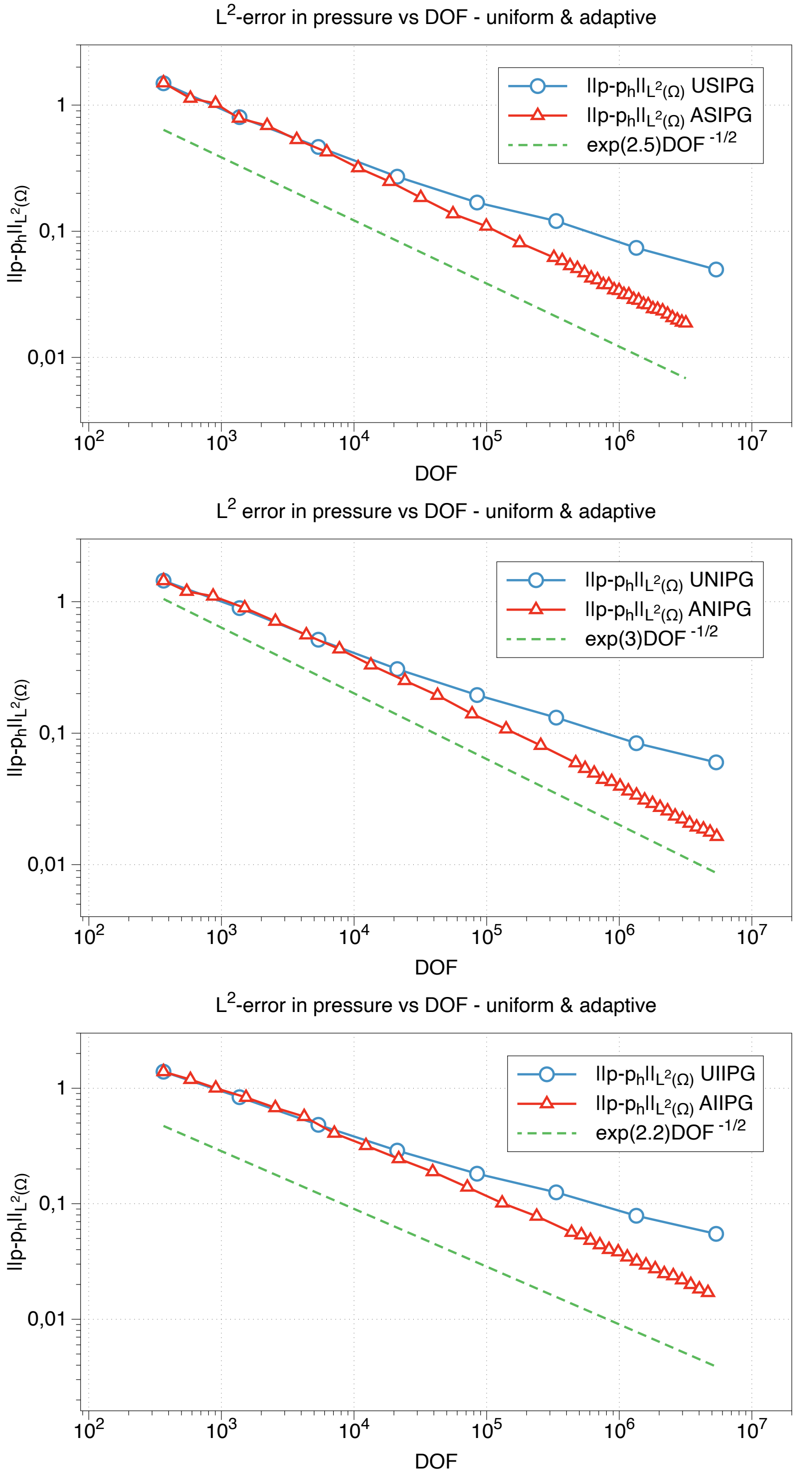

Fig. 5: Pressure L^2-error vs. DOF for SIPG (up), NIPG (center) and IIPG (bottom).

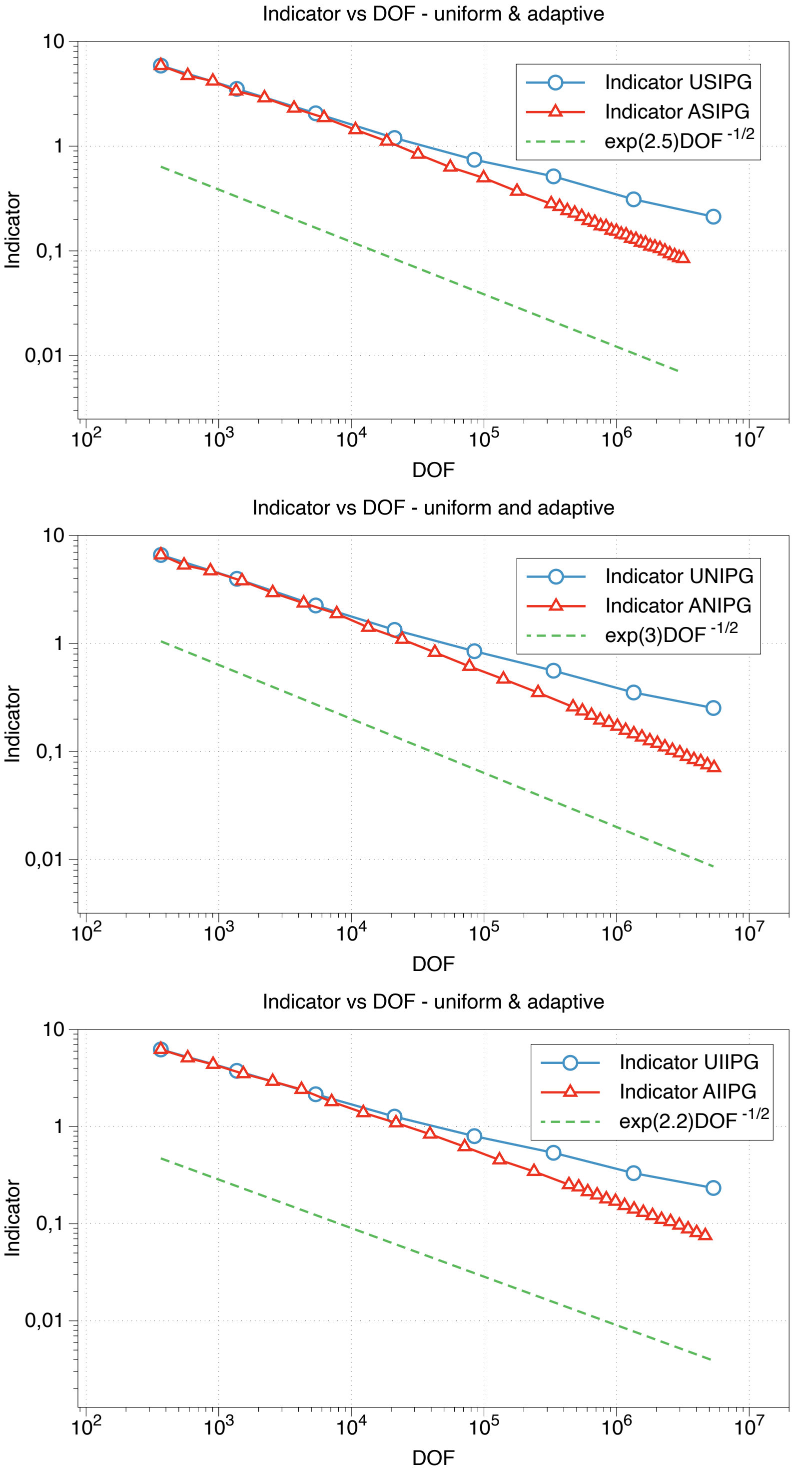

Fig. 6: Global indicator vs. DOF for SIPG (up), NIPG (center) and IIPG (bottom).

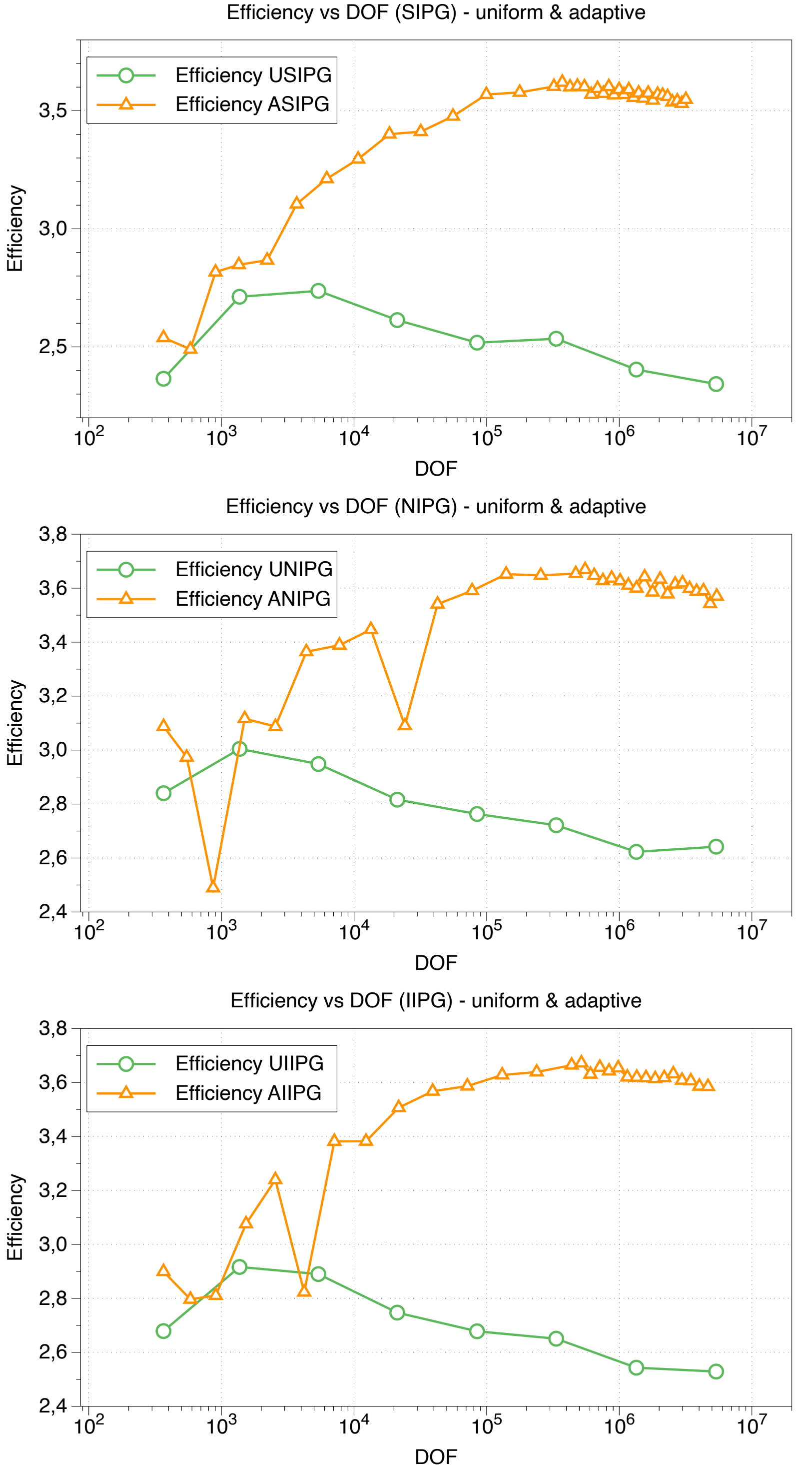

Fig. 7: Efficiency index vs. DOF for SIPG (up), NIPG (center) and IIPG (bottom).

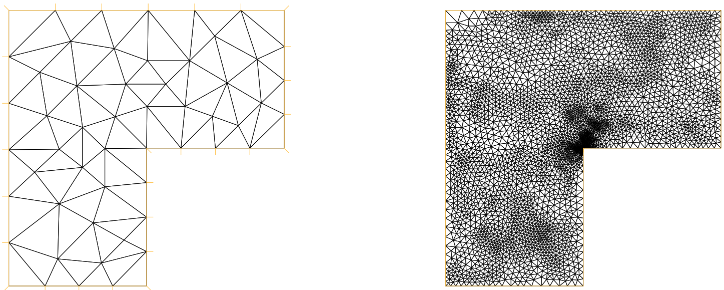

Fig. 8: SIP-EG method: Initial mesh, with 366 DOF (left), and mesh after 9 iterations, with $31\,862$ DOF (right).

6 Appendix

6.1 Approximation of the boundary data

In practical situations, the boundary data $\mathbf{g}_D$ is given by measurements or by the results of a previous computation; in both cases, it is a discrete set of values. To simplify the a posteriori error analysis, it is convenient to assume that this discrete set is interpolated so as to be the trace of a function of $[M_0^k(\mathcal{T}_h)]^d$ on Γ, say $\Pi_h(\mathbf{g}_D)$, and the condition (1) is enforced by adding a correction of the form

$$\mathbf{c}(\mathbf{x}) = -\frac{1}{d\,|\Omega|}\Big(\int_\Gamma \Pi_h(\mathbf{g}_D)\cdot\mathbf{n}\Big)\mathbf{x}. \tag{71}$$

This is adequate since the function $\mathbf{x}$ is a polynomial of degree one, thus is in the discrete space, and its divergence is the constant d, the dimension; clearly,

$$\int_\Gamma \mathbf{x}\cdot\mathbf{n} = \int_\Omega \nabla\cdot\mathbf{x} = d\,|\Omega|.$$

Then the discrete set $\mathbf{g}_D$ is approximated by

$$\mathbf{g}_{h,D} = \Pi_h(\mathbf{g}_D) + \mathbf{c}(\mathbf{x}). \tag{72}$$

By construction, $\mathbf{g}_{h,D}$ satisfies (1), and the discrete problem (8) is solved with the data $\mathbf{g}_{h,D}$. To simplify notation, the index h in $\mathbf{g}_D$ was dropped in the previous analysis.

The same approach is used in the case of a manufactured solution, but in this case we can measure the error made when replacing $\mathbf{g}_D$ with $\mathbf{g}_{h,D}$. For Π_h, we use the Scott–Zhang interpolation operator of degree k in each element, globally continuous. First,

$$\mathbf{g}_{h,D} - \mathbf{g}_D = \Pi_h(\mathbf{g}_D) - \mathbf{g}_D - \frac{1}{d\,|\Omega|}\Big(\int_\Gamma \big(\Pi_h(\mathbf{g}_D) - \mathbf{g}_D\big)\cdot \mathbf{n}\Big)\mathbf{x}.$$

Now,

$$|\mathbf{x}|_{[H^{\frac{1}{2}}(\Gamma)]^d} = \Big(\int_\Gamma\int_\Gamma \frac{|\mathbf{x}-\mathbf{y}|^2}{|\mathbf{x}-\mathbf{y}|^d} d\mathbf{x} d\mathbf{y}\Big)^{\frac{1}{2}},$$

which is a bounded quantity and of course, $\|\mathbf{x}\|_{[L^2(\Gamma)]^d}$ is also a bounded quantity. Therefore the approximation error of $\mathbf{g}_D$ is bounded as follows:

$$\|\mathbf{g}_{h,D} - \mathbf{g}_D\|_{[L^2(\Gamma)]^d} \le \|\Pi_h(\mathbf{g}_D) - \mathbf{g}_D\|_{[L^2(\Gamma)]^d} + \frac{C}{d\,|\Omega|}\|\Pi_h(\mathbf{g}_D) - \mathbf{g}_D\|_{[L^1(\Gamma)]^d},$$

and

$$|\mathbf{g}_{h,D} - \mathbf{g}_D|_{[H^{\frac{1}{2}}(\Gamma)]^d} \le |\Pi_h(\mathbf{g}_D) - \mathbf{g}_D|_{[H^{\frac{1}{2}}(\Gamma)]^d} + \frac{C}{d\,|\Omega|}\|\Pi_h(\mathbf{g}_D) - \mathbf{g}_D\|_{[L^1(\Gamma)]^d}.$$

The a posteriori error analysis developed in the previous sections holds with $\mathbf{g}_{h,D}$ instead of $\mathbf{g}_D$ and $(\mathbf{u}, p)$ replaced by $(\mathbf{u}(h), p(h)) \in H^1(\Omega)^d \times L^2_0(\Omega)$, solution of

$$\begin{cases} -\mu\Delta\mathbf{u}(h) + \nabla p(h) = \mathbf{f} & \text{in } \Omega\,,\\ \nabla\cdot\mathbf{u}(h) = 0 & \text{in } \Omega\,,\\ \mathbf{u}(h) = \mathbf{g}_{h,D} & \text{on } \Gamma\,. \end{cases} \tag{73}$$

As $\mathbf{g}_{h,D}$ is a continuous piecewise polynomial, it belongs to $[H^1(\Gamma)]^d$ and so there exists some s, $0 < s < \frac{1}{2}$, such that $\mathbf{u}(h) \in [H^{1+s}(\Omega)]^d$ and $p(h) \in H^s(\Omega)$. Hence the error equalities of Section 4.1 are well-defined and all reliability and efficiency bounds derived above hold with $\mathbf{u}$ and p replaced by $\mathbf{u}(h)$ and $p(h)$. To express the reliability bounds in terms of $\mathbf{u}$ and p, we use the following:

$$\begin{aligned} |\mathbf{u} - \mathbf{u}(h)|_{[H^1(\Omega)]^d} &\le C\|\mathbf{g}_D - \mathbf{g}_{h,D}\|_{[H^{1/2}(\Gamma)]^d},\\ \|p - p(h)\|_{L^2(\Omega)} &\le C\,\frac{\mu}{\beta}\|\mathbf{g}_D - \mathbf{g}_{h,D}\|_{[H^{1/2}(\Gamma)]^d}. \end{aligned} \tag{74}$$

Regarding efficiency, we must add to the right-hand side of (64) the terms

$$|\mathbf{u} - \mathbf{u}(h)|_{[H^1(E)]^d} \quad \text{and} \quad \|p - p(h)\|_{L^2(E)},$$

and to that of (69),

$$|\mathbf{u} - \mathbf{u}(h)|_{[H^1(\omega_e)]^d} \quad \text{and} \quad \|p - p(h)\|_{L^2(\omega_e)}.$$

These quantities can be bounded by the global estimates in (74), but this is not optimal. Sharper bounds can be derived by applying the localizing techniques of [34], but this is outside the scope of this work.

6.2 Choice of penalty parameters

The penalty parameters σ_e are chosen to guarantee that the form a_ϵ is elliptic in $[V_{h,k}^{EG}]^d$. In the symmetric or incomplete case, we consider an interior edge or face e (the case of a boundary e is simpler) and evaluate $(\nabla \mathbf{u}_h \cdot \mathbf{n}_e, [\mathbf{v}_h])_e$, where $\mathbf{u}_h$ denotes the value of $\mathbf{u}_h$ restricted to one of the elements E adjacent to e,

$$|(\nabla \mathbf{u}_h \cdot \mathbf{n}_e, [\mathbf{v}_h])_e| \leq \|(\nabla \mathbf{u}_h)|_E\|_{[L^2(e)]^{d\times d}} \|[\mathbf{v}_h]\|_{[L^2(e)]^d}.$$

Thus, we must estimate $\|(\nabla \mathbf{u}_h)|_E\|_{[L^2(e)]^{d\times d}}$. In the case of general k, or in the case of quadrilaterals or hexahedra, we use the fact that, after transformation, the function $\nabla \mathbf{u}_h$ belongs to a finite dimensional space in the reference element and apply an equivalence of norms to switch from the surface norm to the volume norm; this brings a constant, say $\hat{D}$, that depends only on d and the degree of the polynomials in the reference element, hence is independent of h. But in the simplex case when $k = 1$, this is trivial because $\nabla \mathbf{u}_h$ is a constant tensor. To simplify, we study this case here but keep in mind that there is an additional constant in the quadrilateral or hexahedral cases. We have

$$\|(\nabla \mathbf{u}_h)|_E\|_{[L^2(e)]^{d\times d}} = \Big(\frac{|e|}{|E|}\Big)^{\frac{1}{2}} \|\nabla \mathbf{u}_h\|_{[L^2(E)]^{d\times d}}.$$

Therefore, when E_1 and E_2 are the two elements sharing e, we have

$$\Big|(\{\nabla \mathbf{u}_h \cdot \mathbf{n}_e\}, [\mathbf{v}_h])_e\Big| \leq$$
$$\leq \frac{1}{2}|e|^{\frac{1}{2}}\Big(\frac{h_e}{\sigma_e}\Big)^{\frac{1}{2}}\Big(\frac{1}{|E_1|}+\frac{1}{|E_2|}\Big)^{\frac{1}{2}} \|\nabla \mathbf{u}_h\|_{[L^2(E_1\cup E_2)]^{d\times d}} \Big(\frac{\sigma_e}{h_e}\Big)^{\frac{1}{2}} \|[\mathbf{v}_h]\|_{[L^2(e)]^d}.$$

Now, we sum over all interior e:

$$\Big|\sum_{e\in\mathcal{E}_h^0}(\{\nabla \mathbf{u}_h \cdot \mathbf{n}_e\}, [\mathbf{v}_h])_e\Big| \leq$$
$$\leq \frac{1}{2}\Big(\int_{\mathcal{E}_h^0} \frac{\sigma_e}{h_e}|[\mathbf{v}_h]|^2\Big)^{\frac{1}{2}} \Big(\sum_{e\in\mathcal{E}_h^0}\frac{h_e}{\sigma_e}|e|\big(\frac{1}{|E_1|}+\frac{1}{|E_2|}\big)\|\nabla \mathbf{u}_h\|^2_{[L^2(E_1\cup E_2)]^{d\times d}}\Big)^{\frac{1}{2}}.$$

Let us take the maximum of the factor

$$\frac{h_e}{\sigma_e}|e|\big(\frac{1}{|E_1|}+\frac{1}{|E_2|}\big) \leq 2\frac{h_e}{\min\sigma_e}\frac{|e|}{\min(|E_1|,|E_2|)},$$

and observe that the second factor is of the order of h_e^{-1}, whatever the dimension. Therefore,

$$\frac{h_e}{\sigma_e}|e|\big(\frac{1}{|E_1|}+\frac{1}{|E_2|}\big) \leq 2\frac{\hat{C}}{\min\sigma_e},$$

where $\hat{C}$ depends only on the regularity of the mesh. It remains to count the number of occurrences of an element E in the sum over e. Each face involves its two adjacent elements. Since a simplex has $d+1$ faces, it is counted $d+1$ times. Therefore,

$$\Big|\sum_{e\in\mathcal{E}_h^0}(\{\nabla \mathbf{u}_h\cdot\mathbf{n}_e\},[\mathbf{v}_h])_e\Big| \le \frac{\sqrt{2(d+1)}}{2}\Big(\frac{\hat{C}}{\min\sigma_e}\Big)^{\frac12}\Big(\int_{\mathcal{E}_h^0}\frac{\sigma_e}{h_e}|[\mathbf{v}_h]|^2\Big)^{\frac12}|\mathbf{u}_h|_h.$$

In the case of a quadrilateral or hexahedral element, $d+1$ is replaced by $2d$, the number of faces, and the constant $\hat{C}$ is multiplied by $\hat{D}$. Of course, this formula is also valid for boundary faces, except that the factor $\frac{\sqrt{2(d+1)}}{2}$ is replaced by 1 and the sums are taken over $\mathcal{E}_h^\partial$. It is used with Young's inequality to deduce the value of $\min\sigma_e$ that guarantees ellipticity of a_ϵ when $\epsilon=0$ or $\epsilon=-1$. When $\epsilon=1$ (non-symmetric case) strictly speaking σ_e could be zero but experiments have shown that the choice $\sigma_e=1$ brings more stability.

6.3 The case of hexahedra with curved faces

From the computer implementation point of view, handling curved faces is more difficult, in particular because the normal vector to each face $\mathbf{n}_e$ is now a function of its position $\mathbf{x}$. But when the family of meshes is regular, this function does not vary much and from a theoretical point of view, all the preceding work applies immediately to regular families of hexahedra with straight edges but non planar faces, with the possible exception of the inf-sup condition. To establish the inf-sup condition in this case, we proceed as in [10], namely use Fortin's Lemma. This amounts to constructing a suitable approximation operator $P_h\in\mathcal{L}([H_0^1(\Omega)]^d;V_{h,k,0}^{EG})$, satisfying for all $\mathbf{v}\in[H_0^1(\Omega)]^d$,

$$b(P_h(\mathbf{v})-\mathbf{v},q_h)=0,\quad \|P_h(\mathbf{v})\|_{EG}\le C|\mathbf{v}|_{[H^1(\Omega)]^d}. \tag{75}$$

In [10], such an operator is constructed by correcting a Scott–Zhang approximation operator, say $\Pi_h\in\mathcal{L}([H_0^1(\Omega)]^d;[M^k(\mathcal{T}_h)\cap H_0^1(\Omega)]^d)$ by means of piecewise constants,

$$P_h(\mathbf{v})=\Pi_h(\mathbf{v})+\mathbf{c}(\mathbf{v}),$$

where $\mathbf{c}(\mathbf{v})$ is a constant vector in each cell. It is shown in [10] that a sufficient condition for the equality in (75) is that $\mathbf{c}(\mathbf{v})$ satisfy on all faces γ_i of E with interior normal $\mathbf{n}_{\gamma_i}$,

$$\int_{\gamma_i}\mathbf{c}(\mathbf{v})\cdot\mathbf{n}_{\gamma_i}=\int_{\gamma_i}\big(\mathbf{v}-\Pi_h(\mathbf{v})\big)\cdot\mathbf{n}_{\gamma_i}. \tag{76}$$

In the case when γ_i is a plane face, (76) reads

$$\mathbf{c}(\mathbf{v}) \cdot \mathbf{n}_{\gamma_i} = \frac{1}{|\gamma_i|} \int_{\gamma_i} \big(\mathbf{v} - \Pi_h(\mathbf{v})\big) \cdot \mathbf{n}_{\gamma_i}. \tag{77}$$

The regularity of the element E implies that this system is solvable provided the maximum number of such faces per element is no more than three in 3-D or two in 2-D and none are opposite faces, in other words, these faces are part of a conical angle. The situation is the same when γ_i is a curved face and the mesh is regular, because the normal vector to a face varies little. In this case (77) is replaced by

$$\mathbf{c}(\mathbf{v}) \cdot \frac{1}{|\gamma_i|} \int_{\gamma_i} \mathbf{n}_{\gamma_i} = \frac{1}{|\gamma_i|} \int_{\gamma_i} \big(\mathbf{v} - \Pi_h(\mathbf{v})\big) \cdot \mathbf{n}_{\gamma_i}. \tag{78}$$

Again, we assume that an element has no more than d faces with interior normals and none are opposite faces. Take the 3-D case of exactly three such faces, say γ_1, γ_2, γ_3. When written in matrix form, (78) reads

$$\mathbf{N}\, \mathbf{c}(\mathbf{v}) = \mathbf{b},$$

where $\mathbf{b}$ is the vector with i-th component

$$\frac{1}{|\gamma_i|} \int_{\gamma_i} \big(\mathbf{v} - \Pi_h(\mathbf{v})\big) \cdot \mathbf{n}_{\gamma_i},$$

and the i-th line of the matrix $\mathbf{N}$ is

$$\mathbf{N}_i = \frac{1}{|\gamma_i|} \int_{\gamma_i} \mathbf{n}_{\gamma_i}^T.$$

Of course, the fact that $\mathbf{n}_{\gamma_i}$ are unit normals imply that $\mathbf{N}$ is uniformly bounded. Moreover, the regularity assumption on the family of triangulations implies that $\mathbf{N}$ is nonsingular and its inverse is uniformly bounded. The second part of (75) follows from this.

Acknowledgment: Part of this work was developed while M.G. was visiting the Laboratoire Jacques-Louis Lions, at Sorbonne Université. M.G. would like to thank Ministerio de Ciencia, Innovación y Universidades (Spain) for its support through grant PRX19/00475; M.G. also acknowledges the support received from the Centro de Investigación de Galicia CITIC, funded by Xunta de Galicia and the European Union (European Regional Development Fund- Galicia 2014-2020 Program), by grant ED431G 2019/01 and to Xunta de Galicia (Spain) by its support through grant GRC ED431C 2018-033. The simulations presented in this paper were carried out in the supercomputer Finisterrae II; the authors would like to thank CESGA for letting them use its capabilities.

References

[1] R. A. Adams and J. J. Fournier, *Sobolev Spaces*, vol. 140 of Pure and Applied Mathematics, Academic Press, New-York, London, 2003.

[2] M. Ainsworth and J. Oden, *A posteriori error estimators for the Stokes and Oseen equations*, SIAM J. Numer. Anal., 34 (1997), pp. 228–245.

[3] A. Allendes, E. Otárola, and A. Salgado, *A posteriori error estimates for the Stokes problem with singular sources*, Comput. Methods Appl. Mech. Engrg., 345 (2019), pp. 1007–1032.

[4] R. Bank and B. Welfert, *A posteriori error estimates for the Stokes problem*, SIAM J. Numer. Anal., 28 (1991), pp. 591–623.

[5] R. Becker, E. Burman, P. Hansbo, and M. Larson, *A reduced P_1-Discontinuous Galerkin Method*, tech. rep., Chalmers Finite Element Centre, Chalmers University of Technology, 2003.

[6] C. Bernardi, V. Girault, and F. Hecht, *A posteriori analysis of a penalty method and applications to the Stokes problem*, Math. Models and Methods in Appl. Sciences, 13 (2003), pp. 1599–1628.

[7] H. Borouchaki, F. Hecht, and P. Frey, *Mesh gradation control*, Int. J. Numer. Meth. Engng., 43 (1998), pp. 1143–1165.

[8] S. Brenner, *Poincaré–Friedrichs inequalities for piecewise H^1 functions*, SIAM J. Numer. Anal., 41 (2003), pp. 306–324.

[9] C. Carstensen and C. Merdon, *Computational survey on a posteriori error estimators for the Crouzeix-Raviart nonconforming finite element method for the Stokes problem*, Computational Methods in Applied Mathematics, 14 (2014), pp. 35–54.

[10] N. Chaabane, V. Girault, B. Riviere, and T. Thompson, *A stable enriched Galerkin element for the Stokes problem*, Applied Numerical Mathematics, 132 (2018), pp. 1–21.

[11] P. G. Ciarlet, *Basic error estimates for elliptic problems*, in Handbook of Numerical Analysis, Vol. II, Handb. Numer. Anal., II, North-Holland, Amsterdam, 1991, pp. 17–351.

[12] E. Creusé and S. Nicaise, *Anisotropic a posteriori error estimation for the mixed discontinuous Galerkin approximation of the Stokes problem*, Numer. Methods Partial Differential Eq., 22 (2006), pp. 449–483.

[13] E. Creusé, S. Nicaise, and G. Kunert, *A posteriori error estimation for the Stokes problem: anisotropic and isotropic discretizations*, Math. Models and Methods in Appl. Sciences, 14 (2004), pp. 1297–1341.

[14] M. Crouzeix and P.-A. Raviart, *Conforming and nonconforming finite element methods for solving the stationary Stokes equations*, R.A.I.R.O. Anal. Numér., 7 R3 (1973), pp. 33–75.

[15] A. Demlow and S. Larsson, *Local pointwise a posteriori gradient error bounds for the Stokes equations*, Math. Comp., 82 (2013), pp. 625–649.

[16] W. Dörfler and M. Ainsworth, *Reliable a posteriori error control for nonconforming finite element approximation of Stokes flow*, Math. Comp., 74 (2005), pp. 1599–1619.

[17] V. Girault and J.-L. Lions, *Two-grid finite-element scheme for the transient Navier–Stokes problem*, Modél. Math. Anal. Numér., 35 (2001), pp. 945–980.

[18] V. Girault, X. Lu, and M. F. Wheeler, *A posteriori error estimates for Biot system using Enriched Galerkin for flow*, Computer Methods in Applied Mechanics and Engineering, (2020).

[19] V. Girault and P.-A. Raviart, *Finite element methods for Navier-Stokes equations. Theory and algorithms*, vol. 5 of Springer Series in Computational Mathematics, Springer-Verlag, Berlin, 1986.

[20] F. Hecht, *New development in FreeFem++*, J. Numer. Math., 20 (2012), pp. 251–265.

[21] P. Houston, D. Schötzau, and T. Wihler, *Energy norm a posteriori error estimation for mixed discontinuous Galerkin approximations of the Stokes problem*, J. Sci. Comp., 22–23 (2005), pp. 347–370.

[22] A. Johnen, J.-C. Weill, and J.-F. Remacle, *Robust and efficient validation of the linear hexahedral element*, Procedia Engineering, 203 (2017), pp. 271–283.

[23] O. Karakashian and F. Pascal, *A posteriori error estimates for a discontinuous Galerkin approximation of second-order elliptic problems*, SIAM J. Numer. Anal., 41 (2003), pp. 2374–2399.

[24] S. Lee, Y.-J. Lee, and M. F. Wheeler, *A locally conservative enriched Galerkin approximation and efficient solver for elliptic and parabolic problems*, SIAM Journal on Scientific Computing, 38 (2016), pp. A1404–A1429.

[25] S. Lee, A. Mikelic, M. Wheeler, and T. Wick, *Phase-field modeling of proppant-filled fractures in a poroelastic medium*, Comp. Meth. in App. Mech. and Eng., 312 (2016), pp. 509–541.

[26] S. Lee and M. Wheeler, *Adaptive enriched Galerkin methods for miscible displacement problems with entropy residual stabilization*, J. Comp. Phys., 331 (2017), pp. 19–37.

[27] ———, *Enriched Galerkin methods for two-phase flow in porous media with capillary pressure*, Journal of Computational Physics, 367 (2017).

[28] R. Rannacher and S. Turek, *Simple nonconforming quadrilateral Stokes*

element, Numerical Methods for Partial Differential Equations, 8 (1992), pp. 97–111.

[29] B. Rivière, *Discontinuous Galerkin Methods for Solving Elliptic and Parabolic Equations: Theory and Implementation*, SIAM, 2008.

[30] L. R. Scott and S. Zhang, *Finite element interpolation of nonsmooth functions satisfying boundary conditions*, Mathematics of Computation, 54 (1990), pp. 483–493.

[31] S. Sun and J. Liu, *A locally conservative finite element method based on piecewise constant enrichment of the continuous Galerkin method*, SIAM Journal on Scientific Computing, 31 (2009), pp. 2528–2548.

[32] R. Verfürth, *A posteriori error estimators for the Stokes equations*, Numer. Math., 55 (1989), pp. 309–325.

[33] R. Verfürth, *A Posteriori Error Estimation Techniques for Finite Element Methods*, Oxford Science Publications, 2013.

[34] L. B. Wahlbin, *Local behavior in Finite Element Methods*, in Handbook of Numerical Analysis, Vol. II, Handb. Numer. Anal., II, North-Holland, Amsterdam, 1991, pp. 353–522.